Gli Transcriptional Activity Is Essential for Kras-Induced Pancreatic Tumorigenesis and Regulates IKBKE/NF-\(\kappa\)B Activity in the Tumor Epithelium

Gli transcriptional activity is essential for Kras-induced pancreatic tumorigenesis and regulates IKBKE/ NF-κB activity in the tumor epithelium

Mihir Rajurkar[1], Wilfredo E. de Jesus-Monge[2], David R. Driscoll[2], Victoria A. Appleman[2], He Huang[1], Jennifer L. Cotton[1], David S. Klimstra[3], Lihua J. Zhu[2], Karl Simin[1], Lan Xu[4], Andrew P. McMahon[5], Brian C. Lewis[2,4,6,7], and Junhao Mao[1,6,7]

[1]Department of Cancer Biology, [2]Program in Gene Function and Expression, [4]Program in Molecular Medicine, and [6]Cancer Center, University of Massachusetts Medical School, Worcester, MA 01605; [3]Department of Pathology, Memorial Sloan-Kettering Cancer Center, New York, NY 10021, [5]Department of Molecular and Cellular Biology and Harvard Stem Cell Institute, Harvard University, Cambridge, MA 02138.

[7]Correspondence should be addressed to JM (junhao.mao@umassmed.edu) or BCL (brian.lewis@umassmed.edu).

Running title: Gli activity in pancreatic tumorigenesis

ABSTRACT

Pancreatic ductal adenocarcinoma (PDAC), one of the most aggressive human malignances, is thought to be initiated by *KRAS* activation. Here we find that transcriptional activation mediated by the Gli family of transcription factors, although dispensable for pancreatic development, is required for Kras-induced proliferation and survival in primary pancreatic epithelial cells in culture, and Kras-driven pancreatic intraepithelial neoplasia and PDAC formation *in vivo*. Further, ectopic Gli1 activation in the mouse pancreas accelerates Kras-driven tumor formation, underscoring the importance of Gli transcription factors in pancreatic tumorigenesis. Interestingly, we demonstrate Gli-stimulated IKBKE (IKKε)/nuclear factor-kappaB (NF-κB) activity in pancreatic cancer cells in culture and *in vivo*, and show that this activity is a critical downstream mediator for Gli-dependent PDAC cell transformation and survival. Together, these studies demonstrate for the first time the requirement for Gli in Kras-dependent pancreatic epithelial transformation, implicate a novel mechanism of Gli-NF-κB oncogenic activation, and provide genetic evidence supporting the therapeutic targeting of Gli activity in pancreatic cancer.

\body

INTRODUCTION

Pancreatic ductal adenocarcinoma (PDAC) is the fourth leading cause of cancer mortality in the United States, with a 5-year survival rate of less than 5% (1, 2). PDAC is thought to arise from precursor lesions termed pancreatic intraepithelial neoplasias (PanINs), which are characterized by mutations in *KRAS* and are believed to be initiating events in this cancer (3, 4). The importance of activating *KRAS* mutations in PDAC development is further underscored by studies of mouse models of the disease (5-7). Thus, understanding of the molecular and genetic mechanisms in Kras-dependent pancreatic tumorigenesis is essential for the development of early diagnostic and treatment tools.

The Gli transcription factors - Gli1, Gli2, and Gli3 - are effectors of the Hedgehog (Hh) signaling pathway. In mammalian cells, the Hh ligands bind to the 12-pass transmembrane receptor, Patched1 (Ptch1), leading to activation of the seven-pass membrane protein, Smoothened (Smo). Smo-mediated intracellular signal transduction controls the activity of the Gli proteins, resulting in transcriptional responses in target tissues (8-10). Dysregulation of Hh-Gli signaling is likely involved in multiple aspects of PDAC formation (11-18); yet its exact roles remain poorly characterized. Unlike Hh-related tumors associated with Gorlin syndrome, mutations in cell surface molecules such as Ptch and Smo have not been identified in human pancreatic cancers (11, 19-21). However, Hh ligands are highly expressed in human and mouse PDAC (12, 13, 15, 18), and emerging evidence suggests that the ligands regulate pancreatic tumor development through a paracrine mechanism. In this model, Hh ligands produced by epithelial tumor cells signal to the adjacent stroma, thereby altering the tumor

microenvironment and regulating tumor growth (16, 17, 22, 23). This model is further supported by recent studies demonstrating that neither genetic removal nor activation of *Smo* in the pancreatic epithelium affects Kras-induced pancreatic tumor formation (18, 23). Consistent with this, treatment of a PDAC mouse model with a Smo antagonist led to alterations in the tumor stroma and enhanced tumor response in combination with gemcitabine (17).

Surprisingly, Gli expression within the pancreatic tumor epithelium is maintained despite Smo deletion and does not correlate with Hh ligand levels (18), suggesting a more complex regulation of the pathway. Several recent studies have also shown that Gli1 gene expression in PDAC cells is regulated by oncogenic pathways such as Kras and transforming growth factor beta (TGF-β), independently of Hh ligand input and the canonical intracellular pathway through Ptch and Smo (18, 24). Gli1 is also required for PDAC cell survival and transformation in culture (18), and ectopic activation of Gli2 in the mouse pancreas induces the formation of undifferentiated tumors (14). Interestingly, sequencing of human PDAC specimens identified mutations in genes encoding Gli transcription factors, including *GLI1* and *GLI3* (3). Together, these data suggest a cell-autonomous regulation of Gli activity in pancreatic tumor epithelial cells, independent of Hh ligands. However, the requirement for Gli activation within the tumor epithelium has not been established in vivo, and the underlying molecular consequences of Gli-mediated transcription during pancreatic tumorigenesis remain unexplored.

In this study, we describe the generation of a novel mouse model of epithelium-specific inhibition of Gli transcriptional activity in Kras-induced pancreatic cancer. We find that although blocking Gli-induced transcription does not affect pancreatic development, it

potently inhibits Kras-driven PanIN and PDAC formation. Conversely, ectopic Gli1 expression accelerates Kras-mediated pancreatic tumorigenesis. Using gene expression profiling and functional assays, we identify downstream regulation of the IKBKE/NF-κB pathway as a novel mechanistic link between Gli transcriptional activation and PDAC cell transformation.

RESULTS

Gli activity is not required for pancreatic development

To investigate the role of Gli transcriptional activity in pancreatic development, we used a conditional Rosa26 knock-in allele of Gli3T (*R26-Gli3T*), which allows ectopic expression of Gli3T protein from the ubiquitously expressed *Rosa26* locus following Cre-mediated recombination (25). Gli3T is a C-terminally truncated form of Gli3 that acts as a dominant repressor of Gli transcription. Over-expression of Gli3T specifically inhibits Gli1- and Gli2-dependent gene transcription, but not lymphoid enhancer-binding factor-1 (LEF1) or serum-response-factor (SRF)-mediated gene transcription in cultured NIH3T3 cells (Fig. 1A-C). These results show the specificity and effectiveness of the Gli3T allele in blocking Hh/Gli transcriptional activation.

We crossed *R26-Gli3T* mice to *Ptf1a-Cre* transgenic mice that direct Cre recombinase expression to the epithelial lineages of the mouse pancreas (26). *Ptf1a-Cre;R26-Gli3T* mice were born at the expected frequency, and their pancreata showed normal parenchymal architecture and cytodifferentiation up to the age of 12 months, the longest time examined (n = 10) (Fig. 1E and J). In the *R26-Gli3T* allele, a 3XFlag tag and IRES-

Venus unit are also inserted at the C-terminus of Gli3T to facilitate identification of transgene expression (25). Therefore, we used detection of the Flag tag with immunoblotting (Fig. 1D) and Venus fluorescence on cyrosections (Fig. 1N) to confirm Cre-mediated expression of Gli3T in pancreatic tissue from *Ptf1a-Cre;R26-Gli3T* mice. We analyzed the expression of the endocrine markers insulin and glucagon and the acinar cell marker amylase, and found no significant differences between Gli3T-expressing and control pancreata (Fig. 1F, G, H, K, L and M). These data show that Gli3T inhibition does not affect differentiation of the pancreatic epithelial lineages, and suggest that cell-autonomous Hh-Gli activity is largely dispensable for the proper development of mouse pancreas.

Gli activation is required for Kras-induced PanIN lesion formation

We next investigated the specific role for Gli transcription in regulating Kras-initiated tumor development in vivo. We generated a mouse model in which simultaneous activation of Kras and inhibition of Gli transcription was achieved by breeding mice harboring a conditionally activated Kras allele (*LSL-Kras^{G12D}*) (27) with *Ptf1a-Cre;R26-Gli3T* mice. As reported previously, Cre-mediated activation of the *LSL-Kras^{G12D}* allele in the mouse pancreas results in the development of slowly progressive PanINs (5). At 6 months of age, *Ptf1a-Cre;LSL-KRAS^{G12D}* mice developed early PanIN lesions, most of which were classified histologically as PanIN1A and PanIN1B (Fig. 2A). These lesions showed a high proliferation index, demonstrated by Ki67 immunohistochemistry (IHC), and evidence of epithelial transformation with associated mucin accumulation as detected by Alcian blue staining (Fig. 2C and E). By 12 months of age, the pancreata of

the *Ptf1a-Cre;LSL-Kras^{G12D}* mice displayed evidence of more advanced lesions, including PanIN2 and PanIN3 lesions (Fig. 2G).

In contrast, inhibition of Gli activity resulted in a dramatic reduction in Kras-driven tumorigenesis. *Ptf1a-Cre;LSL-Kras^{G12D};R26-Gli3T* mice (n=15) examined at 6 months and 12 months of age showed a largely normal parenchymal architecture in the pancreas with little evidence of epithelial transformation (Fig. 2B and 2H). Most of the cells in the pancreas were nonproliferating as determined by Ki67 staining, and there was no reactive stroma (Fig. 2D and 2F), suggesting a critical requirement for Gli transcriptional activation in Kras-induced PanIN lesion formation in vivo.

Pancreatic ductal epithelial transformation is a critical step in the development of Kras-initiated PanIN lesions. Thus, we examined the effect of Gli3T expression on Kras-induced phenotypes in primary pancreatic duct epithelial cells (PDECs) in culture. Consistent with our previous work (15), we found that Kras activation induced the proliferation of PDECs and enhanced their survival in response to challenge by apoptotic stimuli (Fig. S1). However, Gli3T expression abrogated Kras-induced PDEC survival after exposure to cycloheximide (Fig. S1A), and also impaired Kras-induced proliferation in PDECs (Fig. S1B). Together, our in vivo and in vitro data suggest that Gli activation is critical for Kras-initiated pancreatic tumorigenesis, potentially by mediating Kras-induced epithelial cell proliferation and survival.

Interestingly, we did detect a few rare PanIN1 lesions in three *Ptf1a-Cre;LSL-Kras^{G12D};R26-Gli3T* mice (Fig. 2H and I). This observation suggests the possibility that the Gli requirement could eventually be overcome, or that the lesions that developed

failed to express Gli3T. To differentiate between these possibilities, we assayed for transgene expression in these lesions. Because of the high background in detecting the Gli3T C-terminal Flag tag with immunofluorescence staining or IHC, we took advantage of the IRES-Venus unit inserted in the *R26-Gli3T* allele that allows detection of transgene expression by Venus fluorescence on cryosections. We found that the lesions from *Ptf1a-Cre;LSL-Kras^{G12D};R26-Gli3T* mice were Venus negative compared to the adjacent normal-appearing islet and acinar tissues (Fig. 2I and J), indicating that the Gli3T transgene was not expressed in these lesions. These results suggest that the development of rare lesions in animals bearing the *R26-Gli3T* allele is probably due to inefficient Cre recombination and the failure to express Gli3T.

Gli activation is required for Kras-dependent PDAC formation

Our data suggest that Gli transcriptional activity is required for Kras-initiated formation of precursor PanIN lesions. To test whether Gli activity is required for progression to adenocarcinoma, we generated compound mice bearing a single floxed *Trp53* allele (28) in addition to the *LSL-Kras^{G12D}*, *R26-Gli3T*, and *Ptf1a-Cre* alleles. Mice negative for the *R26-Gli3T* allele rapidly developed pancreatic carcinomas with a median latency of 111 days (range 85-164 days) (Fig. 3A). These tumors were predominantly moderately- to poorly-differentiated ductal adenocarcinomas that were frequently invasive and metastatic, with dissemination to lymph nodes, the adjacent intestine, liver, peritoneal cavity and lungs (Fig. 3B, panels i-v). Non-tumor-bearing pancreatic tissue displayed acinar atrophy and contained numerous PanINs from PanIN1 to PanIN3 (Fig. 3B, panel I). By contrast, mice bearing the *R26-Gli3T* allele developed carcinomas with a

significantly longer latency, with a median age of 193 days (range 115-270 days), p <0.001 by Log-rank test (Fig. 3A). Histologically, the tumors that developed in the *R26-Gli3T*-positive animals were indistinguishable from those in *R26-Gli3T*-negative mice, and were also commonly metastatic (Fig. 3B, panels vi-ix). Characterization of tumors by immunostaining for Ki67 or the pancreas progenitor marker PDX1, and immunoblotting for AKT and ERK phosphorylation, showed no differences between tumors induced in *R26-Gli3T*-positive and -negative animals (Fig. S2).

Despite the delayed kinetics, the eventual formation of pancreatic tumors in animals bearing the *R26-Gli3T* allele again raises the question whether the tumors that developed failed to express Gli3T, or whether *Trp53* deletion obviates the need for Gli activity, as suggested by a previous study (29). Thus, we assayed for the presence of Gli3T protein in lysates from tumors, and cell lines derived from these tumors, by immunoblotting with an anti-Flag antibody. While Gli3T protein could be readily detected in 293T cells transfected with a Gli3T expression construct (and pancreas tissue from *Ptf1a-Cre;R26-Gli3T* mice, see Fig. 1), Gli3T could not be detected in any of the tumor (Fig. 3C, top panel) or cell line (Fig. 3C, lower panel) lysates. To determine whether these tumors were derived from cells that failed to undergo recombination, we analyzed DNA extracted from tumors and cell lines with PCR primers that differentiate between unrecombined and recombined *R26-Gli3T* alleles. The unrecombined allele was readily detected in all samples isolated from mice carrying the *R26-Gli3T* allele, whereas only one tumor sample tested positive for the presence of the recombined allele (Fig. 3D). Interestingly, a cell line derived from the tumor that tested positive for recombination was negative for the presence of the recombined *R26-Gli3T* allele, suggesting that the

cells in the tumor carrying the recombined allele represented a minority of the sample, or were normal epithelial cells entrapped within the mass of the tumor. Collectively, our data demonstrate that Gli transcriptional activity is required for pancreatic carcinoma development in vivo.

Gli1 accelerates Kras-initiated pancreatic tumorigenesis

Prior work suggested that Kras regulates Gli1 expression in PDAC cells, and Gli1 activity is critical for PDAC cell survival and transformation in vitro (18). However, the tumorigenic activity of Gli1 has not been examined in the pancreas in vivo. Therefore, we used a recently established conditional Rosa26 knock-in allele of Gli1, *R26-Gli1* (30, 31), to ectopically express Gli1 in the mouse pancreas.

Ptf1a-Cre;R26-Gli1 mice were generated and monitored for over 12 months. Gli1 activation alone did not initiate pancreatic tumors, and the pancreatic development and cytodifferentiation appeared normal in *Ptf1a-Cre;R26-Gli1* mice compared to control *R26-Gli1* mice (Fig. S3). However, activation of both Kras and Gli1 within the pancreas dramatically accelerated tumorigenesis. Although the pancreas appeared normal at birth, the health of the triple-transgenic *Ptf1a-Cre;LSL-Kras^{G12D};R26-Gli1* mice deteriorated rapidly, and the majority of the animals were sacrificed between 6 and 12 weeks of age, although few survived to the age of 10 months (Fig. 4A). At 2 months of age, the *Ptf1a-Cre;LSL-Kras^{G12D}* mice demonstrated only few early PanIN1 lesions as reported previously (5), while the vast majority of the pancreas contained well-organized acinar, islet and ductal tissue (Fig. 4C). In contrast, the *Ptf1a-Cre;LSL-Kras^{G12D};R26-Gli1* mice had wide-spread formation of PanIN lesions resulting in almost complete

disruption of normal pancreatic architecture. These lesions showed a variety of nuclear atypia in the ductal epithelium; some corresponding to human PanIN3 lesions (Fig. 4D). Cytokeratin 8 (CK8) staining confirmed the epithelial phenotype (Fig. 4E). A prominent desmoplastic stromal response, confirmed by smooth muscle actin (SMA) staining, was also present (Fig. 4E).

Molecular analysis of the Kras/Gli1 advanced lesions revealed that cell proliferation as measured by Ki67 staining was significantly increased compared to the lesions with Kras activation alone (Fig. 4F and G, and Fig. S4A). Consistent with a previous report (32), we also detected senescence-associated β-galactosidase expression in early PanIN lesions from two-month-old *Ptf1a-Cre;LSL-Kras^{G12D}* mice (Fig. 4H), while high-grade PanIN lesions from age-matched *Ptf1a-Cre;LSL-Kras^{G12D};R26-Gli1* mice did not exhibit detectable senescence-associated β-galactosidase staining (Fig. 4I and Fig. S4B), suggesting escape from Kras^{G12D}-induced growth arrest/senescence. However, we did not detect invasive PDAC in the *Ptf1a-Cre;LSL-Kras^{G12D};R26-Gli1* mice, and metastasis was not observed in any of the mice we examined. Interestingly, we detected large multilocular cystic lesions resembling mucinous cystic neoplasms (Fig. 4J) in two of the *Ptf1a-Cre;LSL-KRAS^{G12D};R26-Gli1* mice, one at 6 weeks of age and the other at 8 months of age, in addition to the PanIN lesions we described above. The cysts from the *Ptf1a-Cre;LSL-Kras^{G12D};R26-Gli1* mice were as large as 2 cm in diameter and lined by columnar epithelial cells, where abundant mucin production was demonstrated by reaction with Alcian blue (Fig. 4K). Immunohistochemistry for estrogen receptor (ER) and progesterone receptor (PR) in these cystic lesions showed the presence of ER or PR positive cells in the stroma (Fig. S4C and D), a key feature of

human mucinous cystic neoplasms. Taken together, these results suggest that Gli1 activation is not sufficient to initiate PDAC, but synergizes with Kras to promote pancreatic tumor formation in vivo.

A Gli-dependent transcriptional program in PDAC cells

The results from our loss-of-function and gain-of-function genetic analyses underscore the functional importance of Gli activation in pancreatic ductal epithelial transformation. However, the Gli-mediated transcriptional program in pancreatic cancer remains largely unexplored.

Panc1 and MiaPaCa2 are human PDAC cell lines that contain activating mutations in *Kras* and require Gli1 activity for survival and maintenance of their oncogenic properties (18). To further examine Gli-mediated transcriptional regulation in these cells, Panc1 or MiaPaCa2 cells were transfected with a Gli3T expression vector, infected with shRNA constructs against Gli1, or treated with a small molecule Gli inhibitor, GANT61. We found that Gli3T effectively blocked Gli-dependent transcriptional activation in the Panc1 or MiaPaCa2 cells (Fig. 5A), consistent with the result that expression of the Gli target genes, *Ptch1* and *Gli1*, was down-regulated in *Ptf1a-Cre;LSL-Kras^{G12D};R26-Gli3T* mouse mutant pancreas (Fig. S5A). In agreement with previous studies(18), we found that inhibition of Gli-mediated transcription by expression of Gli3T, shRNAs against Gli1, or treatment of GANT61, inhibited cell proliferation, increased apoptosis, and impaired anchorage independent growth in these cell lines (Fig. 5B-D, and Fig. S5F-K). Together, these data demonstrated the importance of Gli transcriptional activation in human PDAC cells.

To identify Gli-dependent downstream target genes, we performed gene expression profiling on Gli3T-expressing Panc1 cells and vector controls. We transfected Panc1 cells with a Gli3T-IRES-nuclear GFP expression construct, and 24 hours post-transfection we isolated GFP-positive cells by FACS and performed expression profiling using Affymetrix chips. As expected, we detected upregulation of *Gli3* that likely reflects the expression of the ectopic Gli3T transgene. We identified 265 genes that were significantly downregulated by Gli3T (Table S1); among them, *Ptch1* and *FoxA2* are known transcriptional targets of the Hh-Gli pathway (Fig. 5E). Interestingly, we also identified several genes involved in regulating Ras intracellular signal transduction, including *SOS2* (RasGEF), *RASA1* (RasGAP), *RIN2* and *RASSF4/5* (Fig. 5E), suggesting possible feedback regulation of Kras signaling in cancer cells influenced by Gli activity.

The PI3K/AKT and MEK/ERK pathways are Kras-stimulated signaling pathways that have been implicated in tumorigenesis (33). In our transcriptional profiling, we found that two subunits of *PI3K, PIK3R1* and *PIK3C2B*, were among the genes whose expression was significantly downregulated by Gli3T (Fig. 5E), indicating a possible interaction between Gli and PI3K/AKT signaling. Thus, we further examined the status of these two critical Kras downstream pathways in PDAC cells. We found that Akt phosphorylation was markedly downregulated in Gli3T-expressing Panc1 cells (Fig. 5F), but was elevated in mouse pancreatic tumors with both Kras and Gli1 activation (Fig. 5G and H). In contrast, ERK phosphorylation was not significantly changed in mouse PanIN lesions and human cancer cells upon Gli regulation (Fig. 5F, I and J). These

results are in agreement with a previous report that showed activation of AKT, but not ERK, when an active form of Gli2 was expressed in mouse pancreas (14).

Hh-Gli regulates Wnt signaling in several developmental, tissue regeneration and tumorigenic contexts (16, 34-37). Interestingly, a recent study suggested that Wnt signaling may also be regulated by Hh signaling in pancreatic tumors (38). Thus, we examined the canonical Wnt activity in Panc1 cells where Gli transcription activity was inhibited by Gli3T. Quantitative RT-PCR (qPCR) analysis showed that the expression of a well-established Wnt target gene *AXIN2* was not inhibited by Gli3T expression in Panc1 and MiaPaCa2 cells (Fig. S6). This result is consistent with the absence of Wnt pathway target genes from the list of differentially expressed genes identified by our microarray experiments (Table S1), and the absence of β-catenin nuclear accumulation in the PanIN lesions with both Kras and Gli1 activation (Fig. S6). These data are also consistent with our genetic result that Gli3T expresion did not affect embryonic pancreatic development (Fig. 1), where canonical Wnt signaling plays a prominent role (39, 40). Together, these data suggest that regulation of canonical Wnt signaling may not play a major role in our Gli-dependent pancreatic tumor models.

Gli-mediated regulation of IKBKE and NF-κB activation in pancreatic tumors.

Our gene expression profile analysis detected an enrichment of genes associated with the NF-κB pathway, including *IKBKE* (IKKε), *TRAF1*, *TRAF3IP2* and *NFKBIE* (Fig. 5E). IKBKE (IKKε) is a IκB Kinase (IKK)-related kinase involved in the activation of the NF-κB pathway (41, 42), and was recently identified as a breast cancer oncogene (43).

Importantly, elevated IKBKE expression was recently shown to be a common feature of PDAC(44). Thus, we examined whether IKBKE/NF-κB activation constituted a novel downstream mechanism of Gli transcription in pancreatic cancer.

We first examined whether NF-κB transcriptional activity is regulated by Gli-mediated transcription. Panc1 cells expressing Gli3T, shRNAS against Gli1, or treated with GANT61, exhibited a significantly lower level of NF-κB activity compared to cells expressing a control plasmid as assayed by measuring the activity of a synthetic NF-κB reporter gene (Fig. 6A). Inhibition of Gli transcriptional activation in Panc1 cells also resulted in marked downregulation of IKBKE gene expression as measured by qPCR or immunoblot analysis (Fig. 6B and C). To determine the functional importance of IKBKE in PDAC cells, we used two shRNA constructs against human *IKBKE* to silence IKBKE expression in Panc1 or MiaPaCa2 cells, and confirmed knockdown efficiency by qPCR (Fig. 6D and Fig. S7A). We found that inhibition of IKBKE expression reduced cell numbers, relative to a non-silencing shRNA control, as measured by an MTT assay (Fig. 6F and Fig. S7C). Further, IKBKE knockdown increased apoptosis, as illustrated by caspase 3 cleavage (Fig. 6G and Fig. S7D), and impaired the ability of PDAC cells to form colonies in soft-agar (Fig. 6H and Fig. S7E). Importantly, these phenotypes were rescued by co-expression of a mouse IKBKE expression vector that is resistant to the two shRNAs targeting human *IKBKE* (Fig. 6E-H and Fig. S7B-E). Together, these data indicate that IKBKE is required for the survival and transformation phenotypes of human PDAC cells.

Next, we determined whether IKBKE and NF-κB activity are regulated by Gli-mediated transcription in vivo. RelA is a member of the NF-κB family, and nuclear accumulation of RelA indicates activation of the classical NF-κB pathway. We therefore performed IHC for IKBKE and RelA in tissue samples from *Ptf1a-Cre;LSL-Kras^{G12D}* and *Ptf1a-Cre;LSL-Kras^{G12D};R26-Gli1* mice at the age of 2 months. We found that, compared to those in *Ptf1a-Cre;LSL-Kras^{G12D}* mice, epithelial cells in *Ptf1a-Cre;LSL-Kras^{G12D};R26-Gli1* mice exhibited significantly increased IKBKE expression and nuclear RelA staining (Fig. 6I-L). In summary, these observations demonstrate activation of IKBKE/NF-κB signaling by Gli proteins in PDAC cells, and highlight a potential mechanism for the observed requirement for Gli transcription for PDAC development in vivo.

DISCUSSION

Non-canonical Gli function in pancreatic tumor cells

Non-canonical Gli regulation has been reported and implicated in several oncogenic settings (29, 45-48). A growing body of evidence also suggests a cell-autonomous non-canonical Gli regulation in pancreatic cancer that is distinct from the the Hh ligand-dependent paracrine effect on the tumor stroma (3, 11, 18, 24, 49). Our results here, together with a previous report (14), show that, unlike Smo activation (23), Gli1 or Gli2 activation is able to cooperate with Kras to promote pancreatic tumorigenesis. Moreover, *GLI1* and *GLI3* were recently reported to be mutated in human PDAC-derived cells (3), and the expression of Gli1 and Gli3 can be regulated in Smo-null

mouse pancreatic tumor cells (18). Together, these studies support the non-canonical model, and indicate a broad involvement of Gli mis-regulation in pancreatic cancer.

Using a dominant repressor Gli3T allele that inhibits all Gli-mediated transcriptional activation, we demonstrate for the first time that Gli transcriptional activity is specifically required for pancreatic tumor formation in vivo, although it is dispensable for normal pancreatic development. Importantly, our data show that Gli activity is required not only for pancreatic tumor initiation, but also for the maintenance of established PDAC cells. Given the demonstrated importance of Hh ligands on the desmoplastic stroma, our results suggest that Gli proteins are attractive therapeutic targets(45, 50) in PDAC, as their inhibition would affect both the tumor epithelium and the reactive stroma.

It is currently not well understood why the pancreatic epithelium is refractory to Ptch/Smo-mediated canonical signaling or how Kras potentially regulates Gli expression levels(18, 49, 51); however, recent work points to an interesting potential connection with the primary cilium (52). Significant Gli signal up-regulation was observed within the pancreatic epithelium after disruption of primary cilium (52), a cellular organelle that is intimately associated with Hh-Gli signal transduction (53). Interestingly, another recent study showed that Kras-mediated transformation of the pancreatic duct epithelium correlates the loss of this organelle in PanIN and PDAC cells in vivo (54). Thus, Kras activation may lead to loss of the primary cilium, which could potentially facilitate the Hh ligand-independent activation of Gli activity in tumor epithelium.

Gli1 activation in pancreatic cancer

Our results on the cooperation of Gli1 with Kras provided the first evidence for the in vivo tumorigenic potential of Gli1 in the pancreas. However, it is interesting to note the phenotypic differences between Gli1 and Gli2 activation in pancreatic tumor initiation. Whereas Gli1 is unable to initiate pancreatic tumorigenesis on its own, activation of Gli2 by the CLEG2 allele drives pancreatic neoplasia, albeit the development of undifferentiated tumors that do not progress via PanINs (14). Several possibilities may account for the difference. First, there are differences in the design of the transgenes. The *R26-Gli1* allele (30) allows Cre-dependent expression of the full-length Gli1 protein from the ubiquitously expressed *Rosa26* locus, whereas in the *CLEG2* allele (14), a dominant active version of Gli2, Gli2ΔN, is expressed via control of the *CAGGS* promoter, a highly active hybrid *CMV/β-actin* promoter. Furthermore, Gli2ΔN consists of an N-terminally truncated form of the protein that lacks an N-terminal repressor domain, which may result in resistance to posttranslational regulation (55). Second, different Cre drivers were used in these two studies. Compared to *Ptf1a-Cre* (26), the *Pdx1-Cre* transgene (56) used in the Gli2ΔN study directs Cre expression in earlier embryonic pancreatic progenitor cells. However, it is possible that the phenotypic difference may indeed reflect distinct properties of these two Gli proteins; indeed, differential transcriptional outputs mediated by Gli1 and Gli2 have been reported (57).

However, in the context of Kras-initiated pancreatic tumorigenesis, both Gli1 and Gli2 showed remarkable capacity to accelerate tumor development. Ectopic expression of either Gli1 or Gli2ΔN, together with Kras activation, resulted in the formation of advanced PanIN lesions by 2 months of age. Only minimal early PanIN1A lesions are detected at this age in mice with Kras activation alone. Extensive fibrosis was also

evident in both Gli1/Kras and Gli2ΔN/Kras tumors, a feature similar to desmoplasia observed in human PDAC. Despite the frequent formation of advanced lesions at an early age, we did not observe invasive or metastatic PDAC in the *Ptf1a-Cre;LSL-Kras^{G12D};R26-Gli1* mice that survived to 10 months of age, suggesting the requirement for additional oncogenic alterations, possibly loss of p53 or p16 function (6, 7). Another intriguing possibility is that paracrine signaling of Hh ligands to the reactive stroma is involved in the stimulation of metastasis. It would be interesting to test whether Gli activation, together with Hh ligand up-regulation in postnatal mouse pancreas, may lead to the development of metastatic PDAC.

A unique Gli transcriptional program in PDAC

Despite the importance of Kras in PDAC, the transcriptional output regulated by this signaling in pancreatic cancer cells remains poorly characterized. Our data here, in agreement with prior studies, place Gli transcription factors downstream of Kras in pancreatic cancer, and our gene expression profiling studies potentially describe a non-canonical transcriptional regulation controlled by Gli proteins in PDAC cells. Interestingly, we did not detect down-regulation of typical Hh-Gli mitogenic targets, such as *cyclin D1* and *MYC* that are commonly found in Hh-related tumors (58-60). Although we can not rule out the possibility that Gli3T inhibition may not fully recapitulate the Gli1/2 null phenotypes in PDAC cells, our data support the idea that Gli proteins may exert a unique transcriptional program in pancreatic cancer cells, a notion that is consistent with recent studies that Gli-mediated transcriptional output is highly context dependent (25, 31, 61). Our data also suggest that canonical Wnt signaling is unlikely to

play a major role in Gli-dependent pancreatic epithelial transformation. Instead, we identified a cluster of Gli-dependent genes that are possibly involved in selective feedback regulation of Kras-stimulated signal transduction in PDAC cells. Further, our finding that Gli3T expression in Panc1 cells suppresses Akt phosphorylation, and that Gli activity is required for the elevated expression of the PI3K subunits *PIK3R1* and *PIK3C2B* in these cells, supports the intriguing possibility that Gli proteins may directly, or indirectly, contribute to the selective activation of the PI3K/AKT pathway.

IKBKE and NF-κB activation in pancreatic cancer

NF-κB activity has long been linked to inflammation-related tumorigenesis (62-64). There is also increasing recognition of intrinsic dysregulation of the pathway in solid tumors. Alteration of NF-κB pathway components was a common finding in a recent comprehensive genomic screen of somatic copy-number alterations across human cancers (65). Further, activation of the NF-κB pathway, possibly via non-canonical IKK kinases such as IKBKE and TBK1, has recently been shown to be critical for several epithelial tumors, including breast and lung carcinomas that harbor *KRAS* mutations (42, 43, 66, 67). Our results in human PDAC cells and mouse tumors indicate enhanced NF-κB activity in the tumor epithelium, a finding that is consistent with previous studies on NF-κB activation in human PDAC cells (68, 69). Our data further suggest that the IKK-related kinase, IKBKE, may play an important functional role in PDAC downstream of Gli proteins. IKBKE levels are elevated in pancreatic tumors with concomitant expression of activated Kras and Gli1, and IKBKE knockdown impairs the survival and transformation of PDAC cells. *IKBKE* was recently identified as a breast cancer

oncogene (43), and recent work demonstrated elevated levels in PDAC samples(44). Therefore, it will be interesting to test whether *IKBKE* functions as an oncogene in PDAC as well. Our finding that multiple components of the NF-κB pathway are regulated downstream of Gli3T also suggest a potential link between Kras activation and NF-κB mediated, in part, by Gli transcription factors. Interestingly, while our data show a novel cell-autonomous regulation of IKBKE/NF-κB by Gli, a recent report suggested that Shh ligand production may be regulated by NF-κB activity in PDAC cells (70). Clearly, further in vivo studies are warranted to elucidate the mechanism of, and requirement for, the interplay among these critical pathways in the pathogenesis of pancreatic cancer.

MATERIALS AND METHODS

Mouse strains: *Ptf1a-Cre, LSL-Kras^{G12D}, Trp53^{flox}, R26-Gli3T* and *R26-Gli1* mice have been described before (25-28, 31). *Ptf1a-Cre;LSL-Kras^{G12D}, Ptf1a-Cre;LSL-Kras^{G12D};R26-Gli3T*, and *Ptf1a-Cre;LSL-Kras^{G12D};R26-Gli1* mice were obtained by crossing *LSL-Kras^{G12D}* to *Ptf1a-Cre;R26-Gli3T* or *Ptf1a-Cre;R26-Gli1* mice. Offspring from the cross of *LSL-Kras^{G12D};R26-Gli3T* to *Ptf1a-cre;Trp53$^{flox/flox}$* mice were followed longitudinally for tumor development for 270 days. All mouse experiments were performed according to the guidelines of IACUC at University of Massachusetts Medical School.

Tissue collection and histology: Upon euthanasia, primary pancreatic tissues and metastatic lesions were separated in pieces and fixed in 4% paraformaldehyde. For

paraffin sections, tissues were dehydrated, and embedded in paraffin blocks, and cut at a thickness of 6 μm. For frozen sections, tissues were dehydrated in 30% sucrose, and embedded in OCT, and sections were cut at a thickness of 12 μm. For RNA and protein analysis, tissues were flash frozen in liquid nitrogen. Tissue sections (6 μm) were stained with hematoxylin and eosin (H&E) using standard reagents and protocols.

Generation of cell lines from tumor tissue: Pancreatic tumors were dissected, minced, and digested at 37°C in a Hank's balanced salt solution (HBSS) containing 2 mg/mL type V collagenase (Sigma) with agitation. After 20 minutes, the digested material was filtered through a 105-μm nylon mesh, and proteases were inactivated by the addition of DMEM/F12 (Invitrogen) supplemented with 10% fetal bovine serum. The tissue was then washed 3 times in HBSS to remove collagenase. The ductal fragments were plated on plastic dishes precoated with rat tail collagen type 1 (BD Bioscience) for further growth in monolayer.

Immunohistochemistry, immunefluorescence and immunoblotting: For immunohistochemistry, high-temperature antigen retrieval was conducted in Sodium Citrate solution (pH 6.0) on paraffin sections for 30 minutes. Sections were blocked in a buffer containing 5% BSA and 0.1% Triton X-100 in PBS and then incubated overnight at 4^0 C in primary antibodies diluted in blocking buffer. Primary antibodies used were: Ki67 (1:500, Abcam), phospho-AKT (1:50, Cell Signaling), phospho-ERK (1:500, Cell Signaling), IKBKE (1:50, Santa Cruz), RelA (1:50, Santa Cruz), β-Catenin (1:400, BD Transduction), Estrogen receptor (1:1000, Santa Cruz), Progesterone receptor (1:1000, Santa Cruz) and PDX1 (1:5000, gift of Dr. Chris Wright, Vanderbilt University). Signal

detection was accomplished with biotinylated secondary antibodies in the Vectastain ABC kit (Vector Labs).

For immunofluorescence, OCT sections were washed with PBS and incubated in blocking buffer containing 5% sheep serum, 1% FBS and 0.1% Triton X-100 in PBS. Sections were then incubated overnight at 4^0 C in primary antibodies diluted in blocking buffer. Primary antibodies used were: Glucagon (1:3000, gift of Dr. Andrew Leiter, UMMS), Amylase (1:800, Sigma), Insulin (1:100, Abcam), Smooth muscle actin (1:500, Sigma), Cytokeratin-8 (1:100, DSHB). Alexa-Fluor fluorescent conjugated secondary antibodies (Invitrogen) were used for detection at a concentration of 1:500 diluted in blocking buffer. Slides were then mounted in mounting media containing DAPI.

For immunoblotting, primary antibodies used were: FlagM2-HRP (1:1000, Sigma), β-Actin (1:1000, Sigma), phospho-AKT (1:1000, Cell Signalling), phospho-ERK (1:1000, Cell Signaling), AKT (1:1000, Cell Signaling), ERK (1:1000, Cell Signaling), IKBKE (1:1000, Sigma), and Myc (1:1000, DSHB). HRP conjugated secondary antibodies used for detection were obtained from Jackson Laboratories.

Alcian blue staining and senescence-associated β-galactosidase staining: For Alcian blue staining, paraffin sections were hydrated and stained for 30 minutes at room temperature using Alcian blue reagent (IHC World). Sections were counterstained with Nuclear Fast Red. For senescence associated β-galactosidase staining, frozen sections were washed in PBS and stained overnight using Senescence β-galactosidase staining solution (Cell Signaling Technology). Sections were counterstained using eosin.

Cell proliferation, apoptosis and soft-agar assays: Gli3T-expressing GFP positive Panc1 or MiaPaCa2 cells were isolated 24 hours after transfection using flow cytometry. For shRNA knockdown, Panc-1 or MiaPaca2 cells were infected with pLKO based lentiviruses expressing shRNAs, and selected for 4 days using puromycin. For GANT61 inhibition, Panc-1 or MiaPaca2 cells were treated with 5 μM or 10 μM GANT61 dissolved in DMSO.

For MTT-based cell proliferation assay, the cells were seeded at a density of 3000 per well in a 96-well plate, treated with 5 mg/ml MTT 5 days after seeding, and lysed in DMSO 4 hours later. Absorbance was measured at 595 nm. Assay was performed in triplicates, and standard deviation was used to calculate error bars.

For apoptosis assay, cells were plated in chamber slides after cell sorting, drug selection, or GANT61 treatment. Cells were fixed in 4% PFA. Immunostaining with a polyclonal antibody against cleaved caspase 3 (1:400, Cell Signaling) was used as a marker for apoptosis. Apoptotic cells were counted in three wells, and relative apoptosis was measured by comparing number of apoptotic cells with control sample. Standard deviation was used to calculate error bars.

For anchorage-independent growth assay using soft-agar, cells were seeded at a density of 6000 cells/well in a 6-well plate of 0.3% agarose in DMEM media containing 10% FBS. Colonies from 12 fields of view were counted 14 days later. Assays were performed in triplicate. Error bars were calculated using standard deviation between triplicates.

Luciferase reporter analysis: NIH3T3 or Panc1 cells were co-transfected with luciferase reporter constructs, GliBS-Luc (gift of Dr. H. Kondoh, Osaka University), TOPflash (Addgene), SRE-luc (gift of Dr. D. Wu, Yale University), NF-κB-Luc (gift of Dr. F. Chan, UMMS), and expression vectors for Renila luciferase, Gli3T, Gli1, Gli2, Lef1 and CDC42. For Gli1 knockdown, the cells were co-transfected with shRNAs targeting Gli1 along with NF-kB luciferase, and Renila expression plasmids. For GANT61 treatment, the Panc-1 cells were co-transfected with NF-kB reporter, and Renila Luciferase, and then treated with 5 μM or 10 μM GANT61 6 hours post transfection. Luciferase assays were conducted 48 hours after transfection using the dual-luciferase reporter kit (Promega). Assays were conducted in triplicates, and standard deviation was used to calculate error bars.

Detection of recombination at the *R26-Gli3T* locus: Polymerase chain reaction was performed on isolated genomic DNA using the primer pair (Forward: 5'-GTAGTCCAGGGTTTCCTTGATG-3', Reverse: 5'-TGCTACTTCCATTTGTCACGTC-3') for detection of the unrecombined R26-Gli3T allele, and (Forward: 5'-GTAGTCCAGGGTTTCCTTGATG-3', Reverse: 5'-GGACTTTCATCCTCATTGGAAG-3') for detection of the recombined allele. Primers to the native R26 locus were used as a control (Forward: 5'-GGAGCGGGAGAAATGGATATG-3', Reverse: 5'-AAAGTCGCTCTGAGTTGTTAT-3')

Quantitative RT-PCR: cDNA synthesis was conducted using Invitrogen Superscript II kit. Primers used for quantitative RT-PCR were: human IKBKE (Forward: 5'-TGCGTGCAGAAGTATCAAGC-3'; Reverse: 5'-TACAGGCAGCCACAGAACAG-3'), mouse IKBKE (Forward: 5'- GCGGAGGCTGAATCACCAG-3'; Reverse: 5'-

GAAAGCCCGAACGTGTTCTCA-3'), Axin2 (Forward: 5'-AGTGTGAGGTCCACGGAAAC -3'; Reverse: 5'- CTTCACACTGCGATGCATTT-3'), human GAPDH (Forward: 5'-ATGGGGAAGGTGAAGGTCG-3'; Reverse: 5'-GGGGTCATTGATGGCAACAATA-3'), mouse GAPDH (Forward: 5'-AGGCCGGTGCTGAGTATGTC-3'; Reverse: 5'-TGCCTGCTTCACCACCTTCT-3'), β-actin (Forward: 5'- TGACAGGATGCAGAAGGAGA-3'; Reverse: 5'-CTGGAAGGTGGACAGTGAGG-3'), human Gli1 (Forward: 5' CCAGCGCCCAGACAGAG-3';Reverse:5'-GGCTCGCCATAGCTACTGAT-3'), mouse Gli1 (Forward: 5'- GTCGGAAGTCCTATTCACGC-3';Reverse: 5'-CAGTCTGCTCTCTTCCCTGC-3'), human Patched-1 (Forward: 5'-CCACAGAAGCGCTCCTACA-3';5'-CTGTAATTTCGCCCCTTCC-3') and mouse Patched-1 (Forward: 5'-AACAAAAATTCAACCAAACCTC-3';Reverse: 5'-TGTCTTCATTCCAGTTGATGTG-3'). All qPCR assays were conducted in triplicates, and standard deviation was used to calculate error bars.

Gli1 and IKBKE **knockdown:** Panc1 or MiaPaCa2 cells were infected with pLKO-based lentiviruses encoding shRNAs targeting human *Gli1* (shGli1#1: CATCCATCACAGATCGCATTT; shGli1#2: GCTCAGCTTGTGTGTAATTAT), and human *IKBKE* (shIKBKE#1: TGGGCAGGAGCTAATGTTTCG; shIKBKE#2: GAGCATTGGAGTGACCTTGTA). Infected cells were selected in 5 μg/ml puromycin for 4 days. MTT assay, soft agar assay, and Caspase staining for apoptosis were conducted as described previously.

PDEC proliferation and survival: PDECs from *Keratin19-tv-a;R26-Gli3T* double transgenic mice were isolated and cultured as previously described (15). The retroviral constructs *RCAS-GFP* and *RCAS-KrasG12D-IRES-GFP* (15) have been previously described. *RCAS-Cre* was a gift from Eric Holland (Memorial Sloan-Kettering Cancer Center). Isolated PDECs were infected with either *RCAS-KrasG12D-IRES-GFP* or RCAS*GFP*, and subsequently infected with *RCAS-Cre* to induce Gli3T expression, or with *RCAS-GFP* as a control. Cell proliferation and survival assays were performed as previously described (15).

Affymetrix gene chip analysis: Panc-1 cells were transfected with a GFP expressing vector carrying Gli3T (pCIG-Gli3T) or a GFP expressing empty vector (pCIG). GFP positive cells were isolated 24 hours post transfection using flow cytometry. RNA was isolated, labeled and hybridized to mouse GeneST1.0 chips (Affymetrix) according to Affymetrix protocols. Three independent biological samples were used for chip analysis. Statistical analyses were performed using R, a system for statistical computation and graphics (http://www.r-project.org). Genes with adjusted p-value <0.05 and absolute fold change ≥ 1.5 were considered potential targets for further investigation.

ACKNOWLEDGEMENTS

Supported by grants from the Charles H. Hood Foundation and American Cancer Society (120376-RSG-11-040-01-DDC) to JM; the Verville Foundation, and NIH grants CA113896, CA113896-S1, and CA155784 to BCL; NIH grant NS033642 to APM; and NIH training grant T32 CA130807 (WJM). JM and BCL are members of the UMass

DERC (P30 DK32520). The authors thank Jiu-Feng Cai and Victor Adelanwa for technical assistance, Drs. Arthur Mercurio and Eric Baehrecke for critical reading of the manuscript, and members of the Mao and Lewis labs for helpful discussions.

REFERENCES:

1. Bardeesy, N. & DePinho, R.A. (2002) Pancreatic cancer biology and genetics. *Nat Rev Cancer* 2, 897-909.
2. Li, D., Xie, K., Wolff, R. & Abbruzzese, J.L. (2004) Pancreatic cancer. *Lancet* 363, 1049-57.
3. Jones, S. et al. (2008) Core signaling pathways in human pancreatic cancers revealed by global genomic analyses. *Science* 321, 1801-6.
4. Almoguera, C. et al. (1988) Most human carcinomas of the exocrine pancreas contain mutant c-K-ras genes. *Cell* 53, 549-54.
5. Hingorani, S.R. et al. (2003) Preinvasive and invasive ductal pancreatic cancer and its early detection in the mouse. *Cancer Cell* 4, 437-50.
6. Aguirre, A.J. et al. (2003) Activated Kras and Ink4a/Arf deficiency cooperate to produce metastatic pancreatic ductal adenocarcinoma. *Genes Dev* 17, 3112-26.
7. Hingorani, S.R. et al. (2005) Trp53R172H and KrasG12D cooperate to promote chromosomal instability and widely metastatic pancreatic ductal adenocarcinoma in mice. *Cancer Cell* 7, 469-83.
8. McMahon, A.P., Ingham, P.W. & Tabin, C.J. (2003) Developmental roles and clinical significance of hedgehog signaling. *Curr Top Dev Biol* 53, 1-114.
9. Lum, L. & Beachy, P.A. (2004) The Hedgehog response network: sensors, switches, and routers. *Science* 304, 1755-9.
10. Hooper, J.E. & Scott, M.P. (2005)Communicating with Hedgehogs. *Nat Rev Mol Cell Biol* 6, 306-17.
11. Morris, J.P.t., Wang, S.C. & Hebrok, M. (2010) KRAS, Hedgehog, Wnt and the twisted developmental biology of pancreatic ductal adenocarcinoma. *Nat Rev Cancer* 10, 683-95.
12. Berman, D.M. et al. (2003) Widespread requirement for Hedgehog ligand stimulation in growth of digestive tract tumours. *Nature* 425, 846-51.
13. Thayer, S.P. et al. (2003) Hedgehog is an early and late mediator of pancreatic cancer tumorigenesis. *Nature* 425, 851-6.
14. Pasca di Magliano, M. et al. (2006) Hedgehog/Ras interactions regulate early stages of pancreatic cancer. *Genes Dev* 20, 3161-73.
15. Morton, J.P. et al. (2007) Sonic hedgehog acts at multiple stages during pancreatic tumorigenesis. *Proc Natl Acad Sci U S A* 104, 5103-8.

16. Yauch, R.L. et al. (2008) A paracrine requirement for hedgehog signalling in cancer. *Nature* 455, 406-410.
17. Olive, K.P. et al. (2009) Inhibition of Hedgehog signaling enhances delivery of chemotherapy in a mouse model of pancreatic cancer. *Science* 324, 1457-61.
18. Nolan-Stevaux, O. et al. (2009) GLI1 is regulated through Smoothened-independent mechanisms in neoplastic pancreatic ducts and mediates PDAC cell survival and transformation. *Genes Dev* 23, 24-36.
19. Teglund, S. & Toftgard, R. (2010) Hedgehog beyond medulloblastoma and basal cell carcinoma. *Biochim Biophys Acta* 1805, 181-208.
20. Rubin, L.L. & de Sauvage, F.J. (2006) Targeting the Hedgehog pathway in cancer. *Nat Rev Drug Discov* 5, 1026-33.
21. Barakat, M.T., Humke, E.W. & Scott, M.P. (2010) Learning from Jekyll to control Hyde: Hedgehog signaling in development and cancer. *Trends Mol Med* 16, 337-48.
22. Bailey, J.M. et al. (2008) Sonic hedgehog promotes desmoplasia in pancreatic cancer. *Clin Cancer Res* 14, 5995-6004.
23. Tian, H. et al. (2009) Hedgehog signaling is restricted to the stromal compartment during pancreatic carcinogenesis. *Proc Natl Acad Sci U S A* 106, 4254-9.
24. Dennler, S. et al. (2007) Induction of sonic hedgehog mediators by transforming growth factor-beta: Smad3-dependent activation of Gli2 and Gli1 expression in vitro and in vivo. *Cancer Res* 67, 6981-6.
25. Vokes, S.A., Ji, H., Wong, W.H. & McMahon, A.P. (2008) A genome-scale analysis of the cis-regulatory circuitry underlying sonic hedgehog-mediated patterning of the mammalian limb. *Genes Dev* 22, 2651-63.
26. Kawaguchi, Y. et al. (2002) The role of the transcriptional regulator Ptf1a in converting intestinal to pancreatic progenitors. *Nat Genet* 32, 128-34.
27. Tuveson, D.A. et al. (2004) Endogenous oncogenic K-ras(G12D) stimulates proliferation and widespread neoplastic and developmental defects. *Cancer Cell* 5, 375-87.
28. Jonkers, J. et al. (2001) Synergistic tumor suppressor activity of BRCA2 and p53 in a conditional mouse model for breast cancer. *Nat Genet* 29, 418-25.
29. Stecca, B. & Ruiz i Altaba, A. (2009) A GLI1-p53 inhibitory loop controls neural stem cell and tumour cell numbers. *Embo J* 28, 663-76.
30. Vokes, S.A. et al. (2007) Genomic characterization of Gli-activator targets in sonic hedgehog-mediated neural patterning. *Development* 134, 1977-89.
31. Lee, E.Y. et al. (2010) Hedgehog pathway-regulated gene networks in cerebellum development and tumorigenesis. *Proc Natl Acad Sci U S A* 107, 9736-41.
32. Morton, J.P. et al. (2010) Mutant p53 drives metastasis and overcomes growth arrest/senescence in pancreatic cancer. *Proc Natl Acad Sci U S A* 107, 246-51.
33. Downward, J. (2003) Targeting RAS signalling pathways in cancer therapy. *Nat Rev Cancer* 3, 11-22.
34. Yang, S.H. et al. (2008) Pathological responses to oncogenic Hedgehog signaling in skin are dependent on canonical Wnt/beta3-catenin signaling. *Nat Genet* 40, 1130-5.
35. Ulloa, F., Itasaki, N. & Briscoe, J. (2007) Inhibitory Gli3 activity negatively regulates Wnt/beta-catenin signaling. *Curr Biol* 17, 545-50.

36. Alvarez-Medina, R., Le Dreau, G., Ros, M. & Marti, E. (2009) Hedgehog activation is required upstream of Wnt signalling to control neural progenitor proliferation. *Development* 136, 3301-9.
37. Shin, K. et al. (2011) Hedgehog/Wnt feedback supports regenerative proliferation of epithelial stem cells in bladder. *Nature*.
38. Pasca di Magliano, M. et al. (2007) Common activation of canonical Wnt signaling in pancreatic adenocarcinoma. *PLoS One* 2, e1155.
39. Murtaugh, L.C., Law, A.C., Dor, Y. & Melton, D.A. (2005) Beta-catenin is essential for pancreatic acinar but not islet development. *Development* 132, 4663-74.
40. Heiser, P.W., Lau, J., Taketo, M.M., Herrera, P.L. & Hebrok, M. (2006) Stabilization of beta-catenin impacts pancreas growth. *Development* 133, 2023-32.
41. Peters, R.T., Liao, S.M. & Maniatis, T. (2000) IKKepsilon is part of a novel PMA-inducible IkappaB kinase complex. *Mol Cell* 5, 513-22.
42. Shen, R.R. & Hahn, W.C. (2010) Emerging roles for the non-canonical IKKs in cancer. *Oncogene* 30, 631-41.
43. Boehm, J.S. et al. (2007) Integrative genomic approaches identify IKBKE as a breast cancer oncogene. *Cell* 129, 1065-79.
44. Cheng, A. et al. (2011) IkappaB Kinase epsilon expression in pancreatic ductal adenocarcinoma. *Am J Clin Pathol* 136, 60-6.
45. Lauth, M., Bergstrom, A., Shimokawa, T. & Toftgard, R. (2007) Inhibition of GLI-mediated transcription and tumor cell growth by small-molecule antagonists. *Proc Natl Acad Sci U S A* 104, 8455-60.
46. Stecca, B. et al. (2007) Melanomas require HEDGEHOG-GLI signaling regulated by interactions between GLI1 and the RAS-MEK/AKT pathways. *Proc Natl Acad Sci U S A* 104, 5895-900.
47. Ho, L. et al. (2009) Gli2 and p53 cooperate to regulate IGFBP-3- mediated chondrocyte apoptosis in the progression from benign to malignant cartilage tumors. *Cancer Cell* 16, 126-36.
48. Flora, A., Klisch, T.J., Schuster, G. & Zoghbi, H.Y. (2009) Deletion of Atoh1 disrupts Sonic Hedgehog signaling in the developing cerebellum and prevents medulloblastoma. *Science* 326, 1424-7.
49. Ji, Z., Mei, F.C., Xie, J. & Cheng, X. (2007) Oncogenic KRAS activates hedgehog signaling pathway in pancreatic cancer cells. *J Biol Chem* 282, 14048-55.
50. Hyman, J.M. et al. (2009) Small-molecule inhibitors reveal multiple strategies for Hedgehog pathway blockade. *Proc Natl Acad Sci U S A* 106, 14132-7.
51. Lauth, M. et al. (2010) DYRK1B-dependent autocrine-to-paracrine shift of Hedgehog signaling by mutant RAS. *Nat Struct Mol Biol* 17, 718-25.
52. Cervantes, S., Lau, J., Cano, D.A., Borromeo-Austin, C. & Hebrok, M. (2010) Primary cilia regulate Gli/Hedgehog activation in pancreas. *Proc Natl Acad Sci U S A* 107, 10109-14.
53. Goetz, S.C., Ocbina, P.J. & Anderson, K.V. (2009) The primary cilium as a Hedgehog signal transduction machine. *Methods Cell Biol* 94, 199-222.
54. Seeley, E.S., Carriere, C., Goetze, T., Longnecker, D.S. & Korc, M. (2009) Pancreatic cancer and precursor pancreatic intraepithelial neoplasia lesions are devoid of primary cilia. *Cancer Res* 69, 422-30.

55. Sasaki, H., Nishizaki, Y., Hui, C., Nakafuku, M. & Kondoh, H. (1999) Regulation of Gli2 and Gli3 activities by an amino-terminal repression domain: implication of Gli2 and Gli3 as primary mediators of Shh signaling. *Development* 126, 3915-24.
56. Gu, G., Dubauskaite, J. & Melton, D.A. (2002) Direct evidence for the pancreatic lineage: NGN3+ cells are islet progenitors and are distinct from duct progenitors. *Development* 129, 2447-57.
57. Eichberger, T. et al. (2006) Overlapping and distinct transcriptional regulator properties of the GLI1 and GLI2 oncogenes. *Genomics* 87, 616-32.
58. Kenney, A.M. & Rowitch, D.H. (2000) Sonic hedgehog promotes G(1) cyclin expression and sustained cell cycle progression in mammalian neuronal precursors. *Mol Cell Biol* 20, 9055-67.
59. Mill, P. et al. (2005) Shh controls epithelial proliferation via independent pathways that converge on N-Myc. *Dev Cell* 9, 293-303.
60. Mao, J. et al. (2006) A novel somatic mouse model to survey tumorigenic potential applied to the Hedgehog pathway. *Cancer Res* 66, 10171-8.
61. Stecca, B. & Ruiz, I.A.A. (2010) Context-dependent regulation of the GLI code in cancer by HEDGEHOG and non-HEDGEHOG signals. *J Mol Cell Biol* 2, 84-95.
62. Hayden, M.S. & Ghosh, S. (2004) Signaling to NF-kappaB. *Genes Dev* 18, 2195-224.
63. Greten, F.R. et al. (2004) IKKbeta links inflammation and tumorigenesis in a mouse model of colitis-associated cancer. *Cell* 118, 285-96.
64. Pikarsky, E. et al. (2004) NF-kappaB functions as a tumour promoter in inflammation-associated cancer. *Nature* 431, 461-6.
65. Beroukhim, R. et al. (2010) The landscape of somatic copy-number alteration across human cancers. *Nature* 463, 899-905.
66. Barbie, D.A. et al. (2009) Systematic RNA interference reveals that oncogenic KRAS-driven cancers require TBK1. *Nature* 462, 108-12.
67. Meylan, E. et al. (2009) Requirement for NF-kappaB signalling in a mouse model of lung adenocarcinoma. *Nature* 462, 104-7.
68. Holcomb, B., Yip-Schneider, M. & Schmidt, C.M. (2008) The role of nuclear factor kappaB in pancreatic cancer and the clinical applications of targeted therapy. *Pancreas* 36, 225-35.
69. Lu, Z. et al. (2011) miR-301a as an NF-kappaB activator in pancreatic cancer cells. *Embo J* 30, 57-67.
70. Nakashima, H. et al. (2006) Nuclear factor-kappaB contributes to hedgehog signaling pathway activation through sonic hedgehog induction in pancreatic cancer. *Cancer Res* 66, 7041-9.

FIGURE LEGENDS

Figure 1. Gli-induced transcriptional activation is dispensable for pancreatic development. (**A-C**) Gli3T blocks Gli-dependent transcriptional activity. Gli3T inhibits Gli-mediated luciferase reporter activity induced by Gli1 and Gli2 in transfected NIH3T3 cells (A). Gli3T does not inhibit TCF4-induced TopFlash reporter activity (B), or serum response factor-dependent SRE-luciferase reporter activity induced by the CDC42 GTPase (C). Open bars: control cells; black bars: Gli3T-expressing cells. (**D**) Immunoblot detection of Gli3T expression in pancreatic lysates from 6-month-old *R26-Gli3T* and *Ptf1a-Cre;R26-Gli3T* mice using an antibody against the Flag epitope tag. (**E-N**) H&E staining (E and J), immunofluoresence staining of amylase (F and K), glucagon (G and L) and insulin (H and M), and Venus fluorescence (I and N) in pancreata derived from *R26-Gli3T* (E-I) and *Ptf1a-Cre;R26-Gli3T* (J-N) mice.

Figure 2. Gli-mediated transcription is required for Kras-initiated PanIN formation. (**A-F**) Representative histological sections from *Ptf1a-Cre;LSL-Kras^{G12D}* (A, C and E) and *Ptf1a-Cre;LSL-Kras^{G12D};R26-Gli3T* (B, D and F) mice stained with H&E (A and B), Alcian blue (C and D) and an antibody against Ki67 (E and F). (**G-J**) PanIN lesions detected in *Ptf1a-Cre;LSL-Kras^{G12D};R26-Gli3T* mice. H&E staining shows wide-spread advanced PanIN formation in *Ptf1a-Cre;LSL-Kras^{G12D}* pancreata (G), while only rare PanIN1 lesions were detected in a 12-month-old *Ptf1a-Cre;LSL-KRAS^{G12D};R26-Gli3T* mouse (H, I). Note robust Venus fluorescence in adjacent acinar and endocrine cells

indicating expression of Gli3T. The boundary of the lesions from the adjacent slides is delineated by dashed black (I) and white (J) lines.

Figure 3. Gli transcriptional activation is required for PDAC formation. (**A**) Kaplan-Meier survival curve for *Ptf1a-Cre;LSL-Kras^{G12D};Trp53$^{flox/wt}$* mice, *Ptf1a-Cre;LSL-Kras^{G12D};Trp53$^{flox/wt}$;R26-Gli3T* mice, and *Ptf1a-Cre*- and *LSL-Kras^{G12D}*-negative littermate controls. $p < 0.001$ for comparison between *R26-Gli3T*-positive and –negative animals. (**B**) Representative H&E stained histological sections from lesions arising in *Ptf1a-Cre;LSL-Kras^{G12D};Trp53$^{flox/wt}$* (i-v) and *Ptf1a-Cre;LSL-Kras^{G12D};Trp53$^{flox/wt}$;R26-Gli3T* mice (vi-ix). PanIN lesions (i), glandular PDAC (ii), undifferentiated carcinoma (iii), lymph node metastasis (iv), and liver metastasis identified in *Ptf1a-Cre;LSL-Kras^{G12D};Trp53$^{flox/wt}$* mice. Glandular PDAC (vi), undifferentiated carcinoma (vii), liver metastasis (viii) and intestinal invasion (ix) observed in *Ptf1a-Cre;LSL-Kras^{G12D};Trp53$^{flox/wt}$;R26-Gli3T* mice. (**C**) Immunoblotting for Gli3T protein (using an anti-Flag antibody) in lysates from *R26-Gli3T*-positive and -negative tumors (top panel) and cell lines derived from these tumors (bottom panel). (**D**) PCR of genomic DNA to detect the recombination status of the *R26-Gli3T* allele in *R26-Gli3T*-positive tumor samples. Amplification of the native *Rosa26* locus was used as a control.

Figure 4. Gli1 promotes Kras-initiated pancreatic tumorigenesis. (**A**) Survival of *Ptf1a-Cre;LSL-Kras^{G12D};R26-Gli1* mice is significantly less than that of *Ptf1a-Cre;LSL-Kras^{G12D}* and *Ptf1a-Cre;R26-Gli* mice. (**B-D**) H&E staining of panceata derived from 2-

month-old *Ptf1a-Cre;R26-Gli1* (B), *Ptf1a-Cre;LSL-Kras^{G12D}* (C) and *Ptf1a-Cre;LSL-Kras^{G12D};R26-Gli1* (D) mice. (**E**) Immunostaining for cytokeratin 8 (red) and α-smooth muscle actin (green) in a *Ptf1a-Cre;LSL-Kras^{G12D};R26-Gli1* derived pancreatic lesion. (**F** and **G**) IHC for Ki67 in *Ptf1a-Cre;LSL-Kras^{G12D}* (F) and *Ptf1a-Cre;LSL-Kras^{G12D};R26-Gli1* (G) pancreata. (**H** and **I**) Senescence-associated β-galactosidase staining of pancreatic lesions from *Ptf1a-Cre;LSL-Kras^{G12D}* (H) and *Ptf1a-Cre;LSL-Kras^{G12D};R26-Gli1* (I) mice. (**J**) H&E staining of pancreatic cystic lesions from a 1-month-old *Ptf1a-Cre;LSL-Kras^{G12D};R26-Gli1* mouse. (**K**) Alcian blue staining revealing abundant mucin production in epithelial cells in the cysts.

Figure 5. Gli-mediated transcriptional program in pancreatic cancer cells. (**A**) Changes in Gli-luciferase reporter activity in Gli3T-expressing and control Panc1 (black bars) and MiaPaCa2 (gray bars) cells. (**B**) Cell proliferation, measured by MTT assay, (**C**) apoptosis, and (**D**) anchorage-independent soft agar colony formation by FACS-isolated Gli3T-expressing and control Panc1 (black bars) and MiaPaCa2 (gray bars) cells. (**E**) Heat map illustrating mRNA expression of selected genes in Gli3T-expressing and control Panc1 cells. Red, high expression; green, low expression. (**F**) Immunoblot analysis of the levels of AKT phosphorylation (p-AKT), total AKT, ERK phosphorylation (p-ERK), and total ERK, in isolated Gli3T-expressing and control Panc1 cells. (**G-J**) IHC for p-AKT (G and H) and p-ERK (I and J) in pancreatic lesions from *Ptf1a-Cre;LSL-Kras^{G12D}* (G and I) and *Ptf1a-Cre;LSL-Kras^{G12D};R26-Gli1* (H and J) mice at 2 months of age.

Figure 6. Gli regulates IKBKE and NF-κB activity in pancreatic cancer cells. (**A**) Inhibition of NF-κB reporter activity by Gli3T, shRNAs against Gli1, and GANT61 in Panc1 cells 48 hours after transfection. (**B**) qPCR analysis of *IKBKE* mRNA expression in response to Gli3T expression, Gli1 knockdown, and GANT61 treatment. (**C**) Immunoblot analysis of IKBKE expression in control and Gli3T-expressing Panc1 cells. (**D**) qPCR analysis of *IKBKE* mRNA level in Panc1 cells expressing shRNA constructs against GFP (control) or IKBKE (shIKBKE #1 and shIKBKE #2). **(E)** Immunoblot analysis for expression of myc-tagged mouse IKBKE (mIKBKE) in Panc1 cells expressing shRNA constructs against human *IKBKE*. Cell proliferation (**F**), apoptosis **(G)** and soft agar colony formation (**H**) in Panc1 cells expressing shRNA constructs against *GFP* or *IKBKE* with or without mouse IKBKE expression. IHC staining of IKBKE (**I, J**) and RelA (**K,L**) in pancreatic lesions from *Ptf1a-Cre;LSL-Kras*^{G12D} **(I,K)** and *Ptf1a-Cre;LSL-Kras*^{G12D}*;R26-Gli1* **(J, L)** mice. Note the predominantly cytoplasmic staining of RelA in panel J, and increased nuclear staining in panel K.

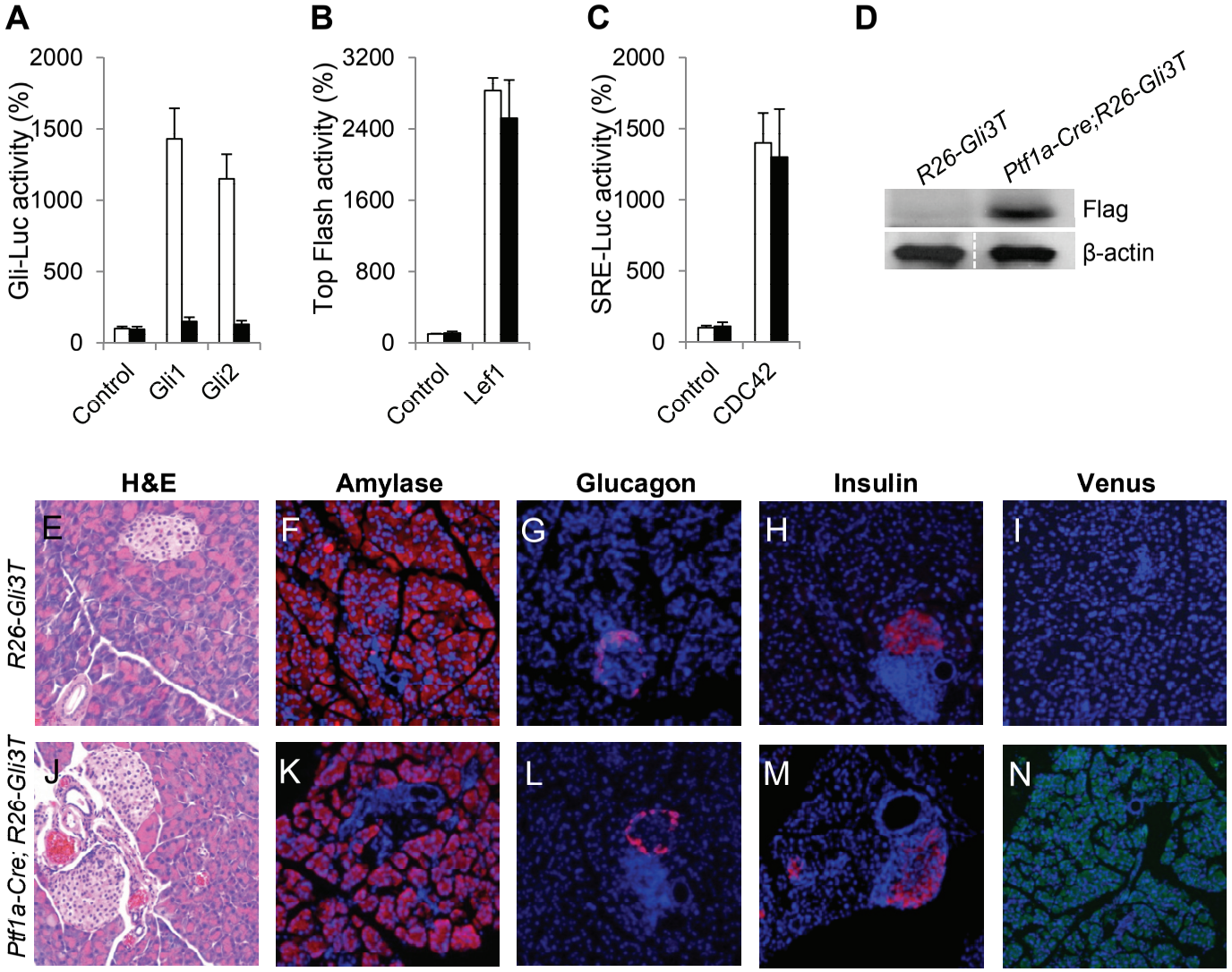
A
Gli-Luc activity (%)
2000
1500
1000
500
0
Control
Gli1
Gli2
B
Top Flash activity (%)
3200
2400
1600
800
0
Control
Lef1
C
SRE-Luc activity (%)
2000
1500
1000
500
0
Control
CDC42
D
R26-Gli3T
Ptf1a-Cre;R26-Gli3T
Flag
β-actin
H&E
Amylase
Glucagon
Insulin
Venus
R26-Gli3T
Ptf1a-Cre; R26-Gli3T
E
F
G
H
I
J
K
L
M
N

Figure 1

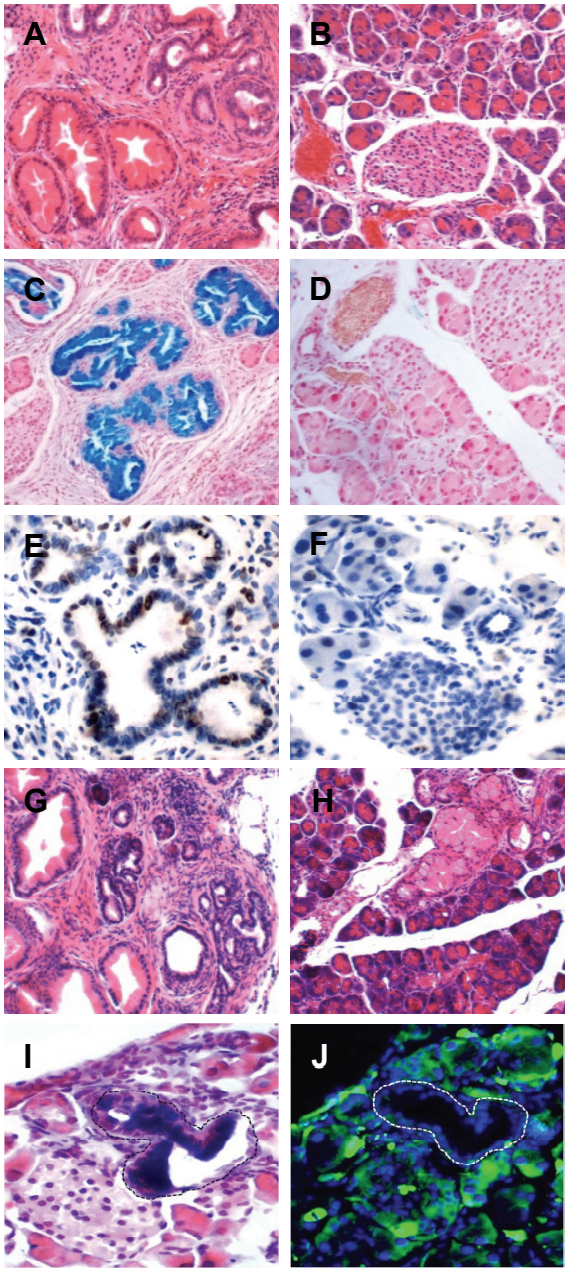

Figure 2

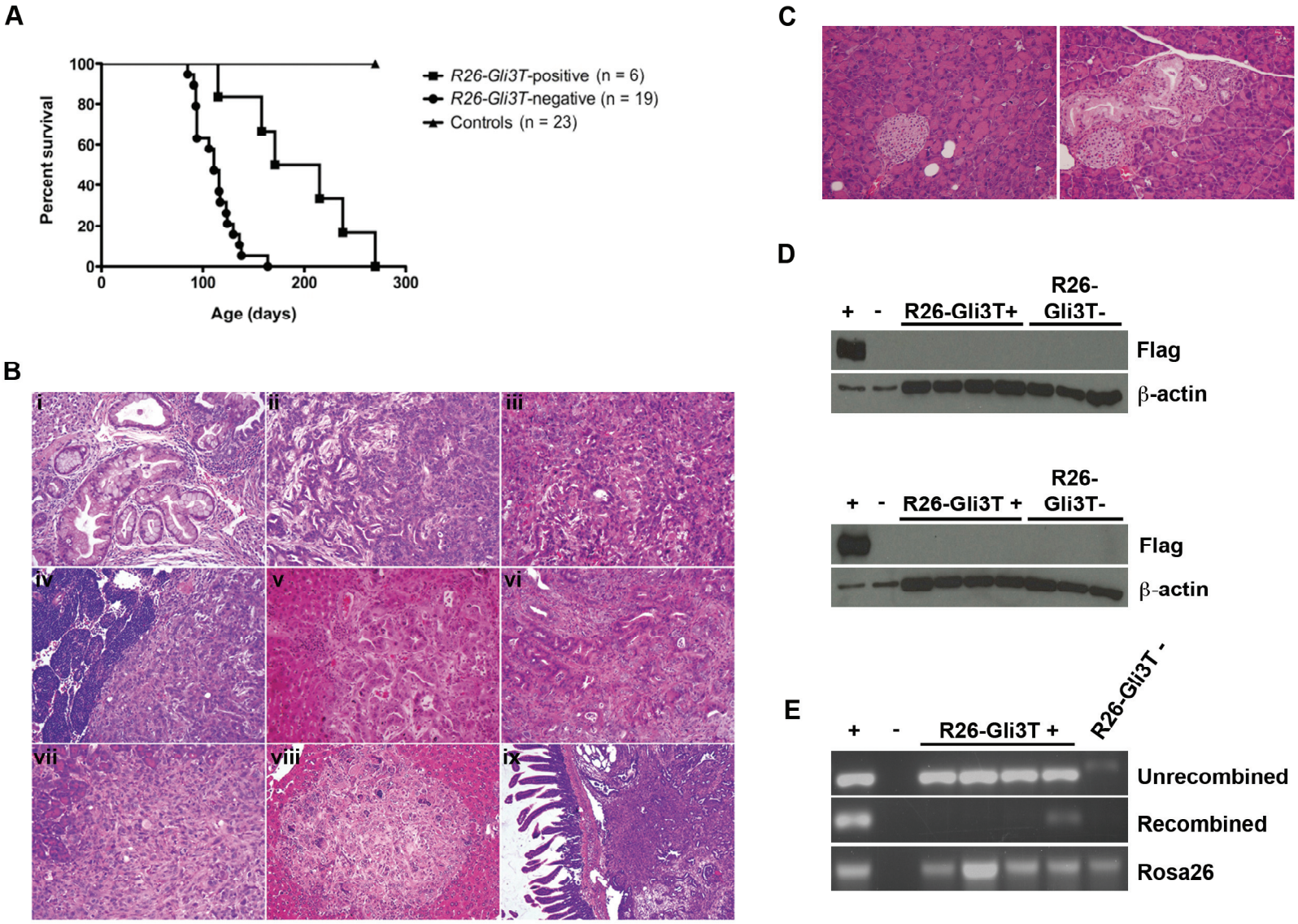
A
Percent survival
100
80
60
40
20
0
0
100
200
300
Age (days)
R26-Gli3T-positive (n = 6)
R26-Gli3T-negative (n = 19)
Controls (n = 23)
B
i
ii
iii
iv
v
vi
vii
viii
ix
C
D
+
-
R26-Gli3T+
R26-Gli3T-
Flag
β-actin
+
-
R26-Gli3T +
R26-Gli3T-
Flag
β-actin
E
+
-
R26-Gli3T +
R26-Gli3T -
Unrecombined
Recombined
Rosa26

Figure 3

Figure 3. Gli transcriptional activation is required for PDAC formation. (A) Kaplan-Meier survival curve for *Ptf1a-Cre;LSL-Kras^{G12D};Trp53$^{flox/wt}$*, *Ptf1a-Cre;LSL-Kras^{G12D};Trp53$^{flox/wt}$;R26-Gli3T*, and *Ptf1a-Cre-* and *LSL-Kras^{G12D}*-negative littermate control mice. $p < 0.001$ for comparison between *R26-Gli3T*-positive and –negative animals. **(B)** Representative histological sections from lesions arising in *Ptf1a-Cre;LSL-Kras^{G12D};Trp53$^{flox/wt}$* (i-v) and *Ptf1a-Cre;LSL-Kras^{G12D};Trp53$^{flox/wt}$;R26-Gli3T* mice (vi-ix). PanIN lesíons (i), glandular PDAC (ii), undifferentiated carcinoma (iii), lymph node metastasis (iv), and liver metastasis (v) identified in *Ptf1a-Cre;LSL-Kras^{G12D};Trp53$^{flox/wt}$* mice. Glandular PDAC (vi), undifferentiated carcinoma (vii), liver metastasis (viii) and intestinal invasion (ix) observed in *Ptf1a-Cre;LSL-Kras^{G12D};Trp53$^{flox/wt}$;R26-Gli3T* mice. **(C)** H&E stained histological sections from the pancreas of a 4-month old *Ptf1a-Cre;LSL-Kras^{G12D};Trp53$^{flox/wt}$;R26-Gli3T* mouse, a time at which PDAC is commonly observed in *Ptf1a-Cre;LSL-Kras^{G12D};Trp53$^{flox/wt}$* littermates. **(D)** Immunoblotting for Gli3T protein (using an anti-Flag antibody) in lysates from *R26-Gli3T*-positive and -negative tumors (top panel) and cell lines derived from these tumors (bottom panel). **(E)** PCR of genomic DNA to detect the recombination status of the *R26-Gli3T* allele in *R26-Gli3T*-positive tumor samples. Amplification of the native *Rosa26* locus was used as a control.

Figure 3

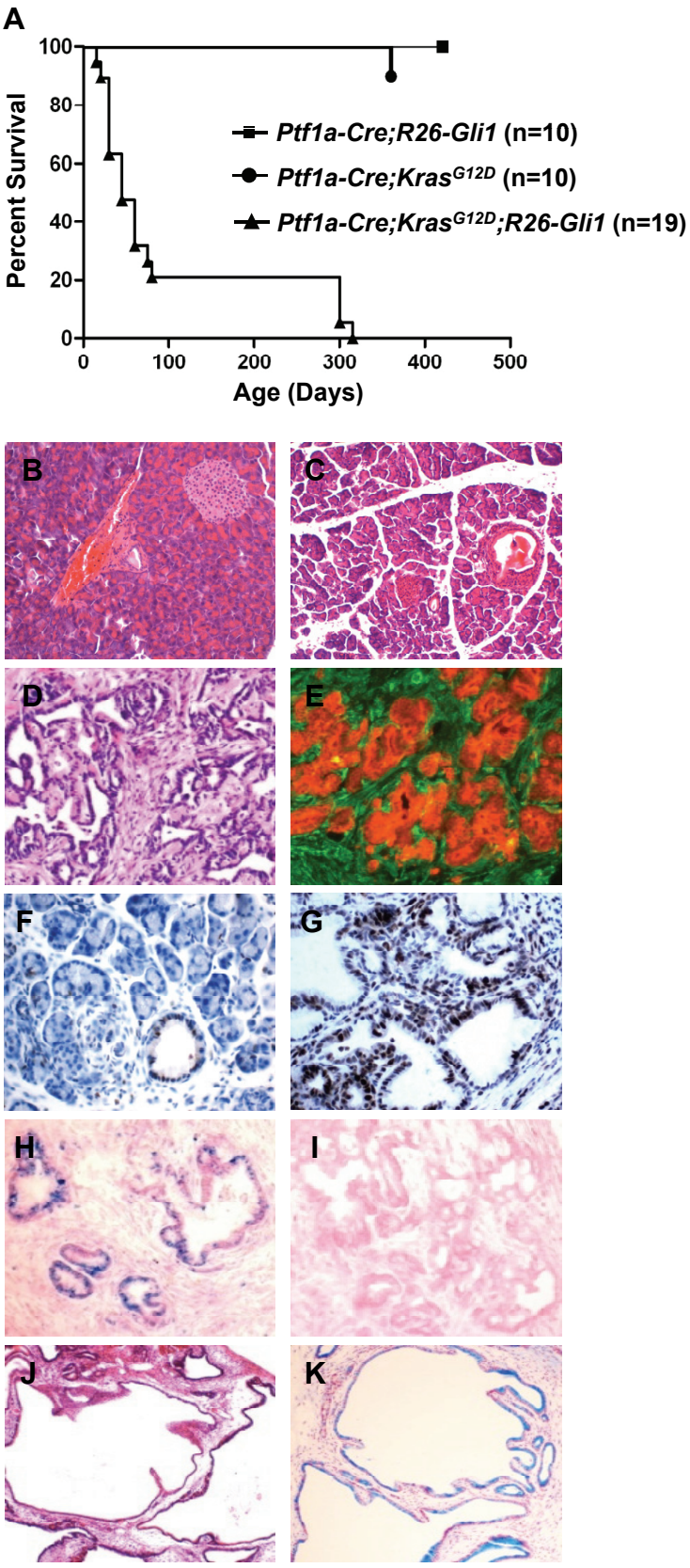
A
100
80
60
40
20
0
Percent Survival
0
100
200
300
400
500
Age (Days)
Ptf1a-Cre;R26-Gli1 (n=10)
Ptf1a-Cre;KrasG12D (n=10)
Ptf1a-Cre;KrasG12D;R26-Gli1 (n=19)
B
C
D
E
F
G
H
I
J
K

Figure 4

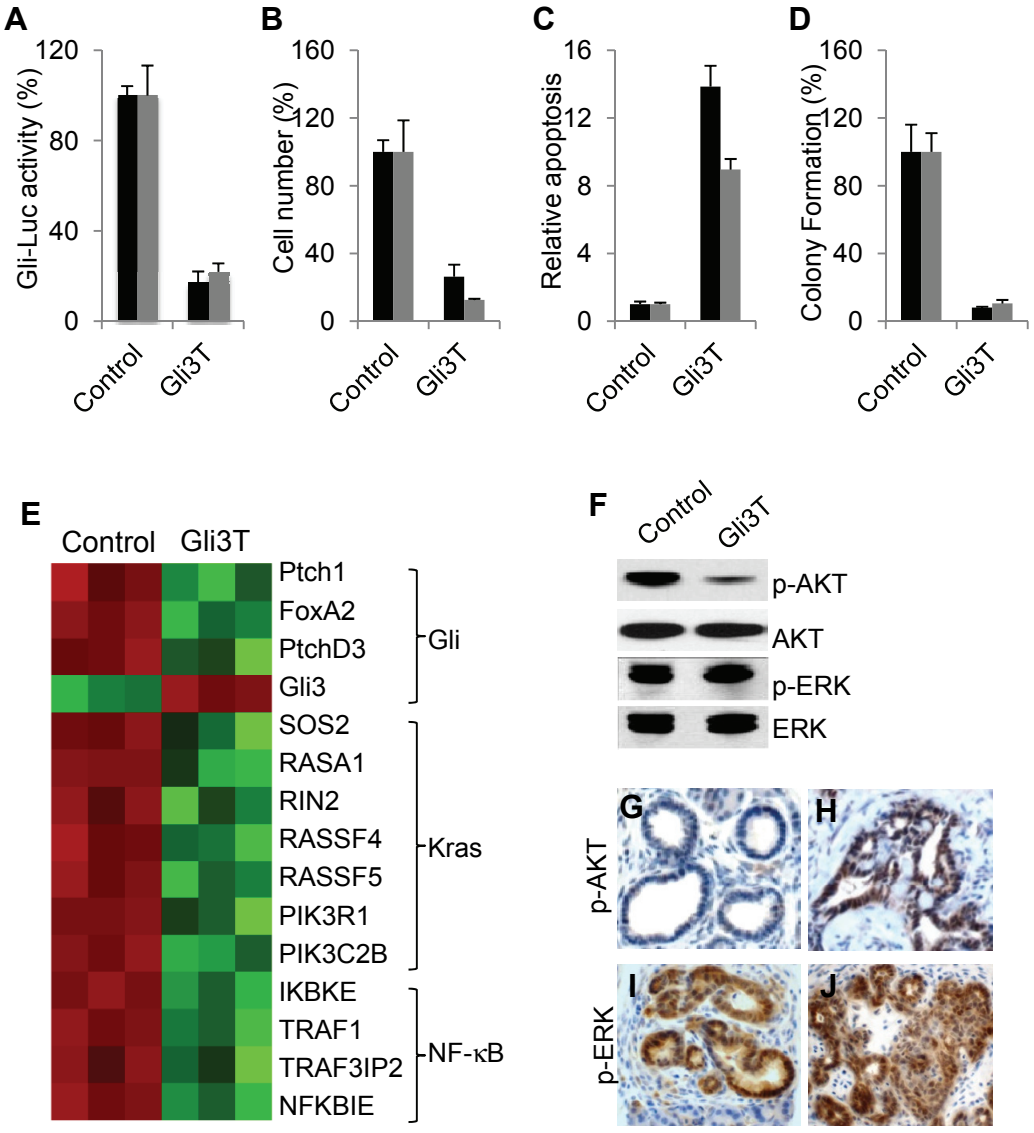
A
Gli-Luc activity (%)
120
80
40
0
Control
Gli3T
B
Cell number (%)
160
120
80
40
0
Control
Gli3T
C
Relative apoptosis
16
12
8
4
0
Control
Gli3T
D
Colony Formation (%)
160
120
80
40
0
Control
Gli3T
E
Control
Gli3T
Ptch1
FoxA2
PtchD3
Gli3
Gli
SOS2
RASA1
RIN2
RASSF4
RASSF5
PIK3R1
PIK3C2B
Kras
IKBKE
TRAF1
TRAF3IP2
NFKBIE
NF-κB
F
Control
Gli3T
p-AKT
AKT
p-ERK
ERK
G
H
p-AKT
I
J
p-ERK

Figure 5

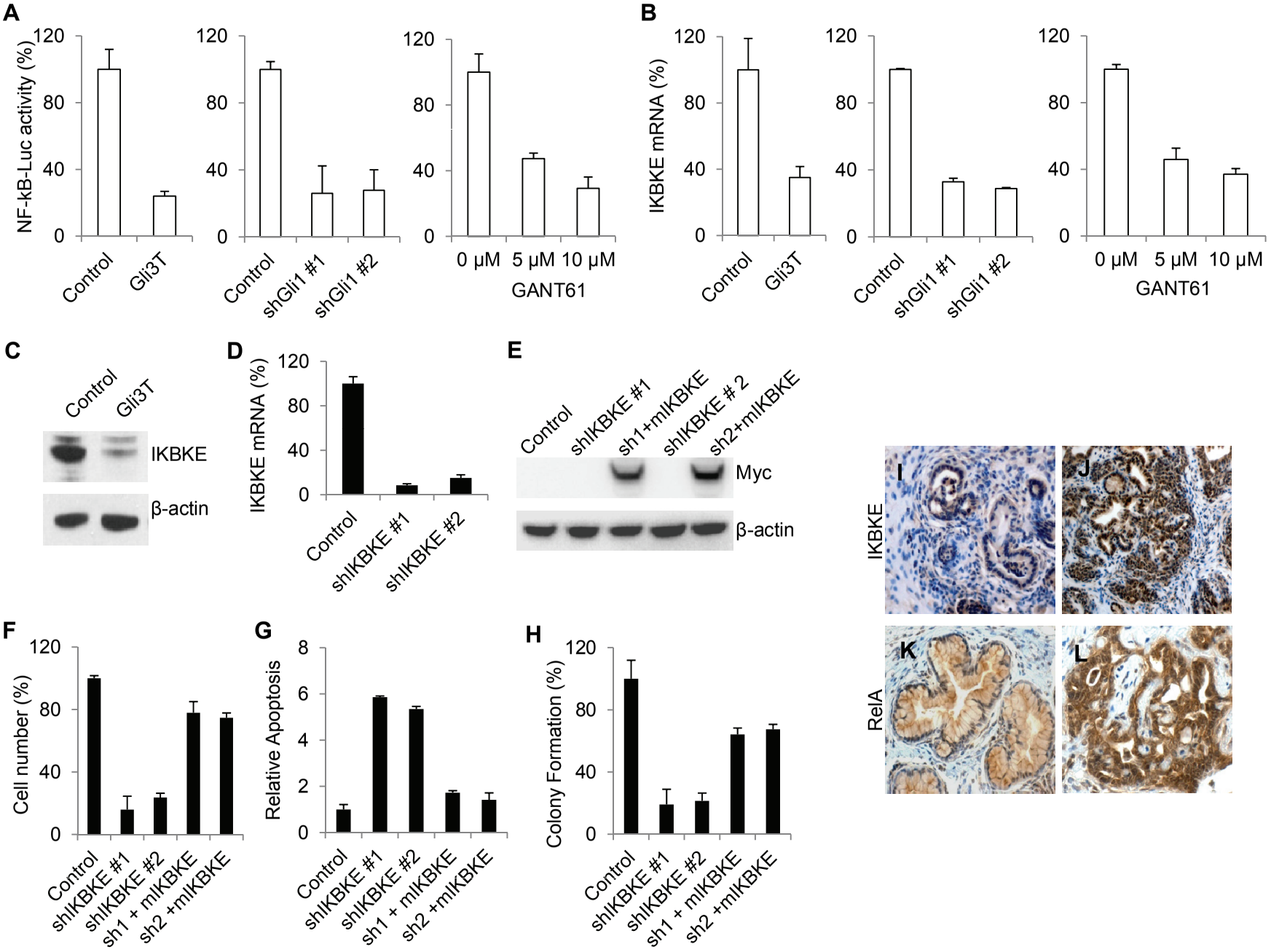
A
NF-kB-Luc activity (%)
120
80
40
0
Control
Gli3T
Control
shGli1 #1
shGli1 #2
0 μM
5 μM
10 μM
GANT61
B
IKBKE mRNA (%)
Control
Gli3T
Control
shGli1 #1
shGli1 #2
0 μM
5 μM
10 μM
GANT61
C
Control
Gli3T
IKBKE
β-actin
D
IKBKE mRNA (%)
Control
shIKBKE #1
shIKBKE #2
E
Control
shIKBKE #1
sh1+mIKBKE
shIKBKE # 2
sh2+mIKBKE
Myc
β-actin
IKBKE
I
J
RelA
K
L
F
Cell number (%)
Control
shIKBKE #1
shIKBKE #2
sh1 + mIKBKE
sh2 +mIKBKE
G
Relative Apoptosis
8
6
4
2
0
Control
shIKBKE #1
shIKBKE #2
sh1 + mIKBKE
sh2 +mIKBKE
H
Colony Formation (%)
Control
shIKBKE #1
shIKBKE #2
sh1 + mIKBKE
sh2 +mIKBKE

Figure 6

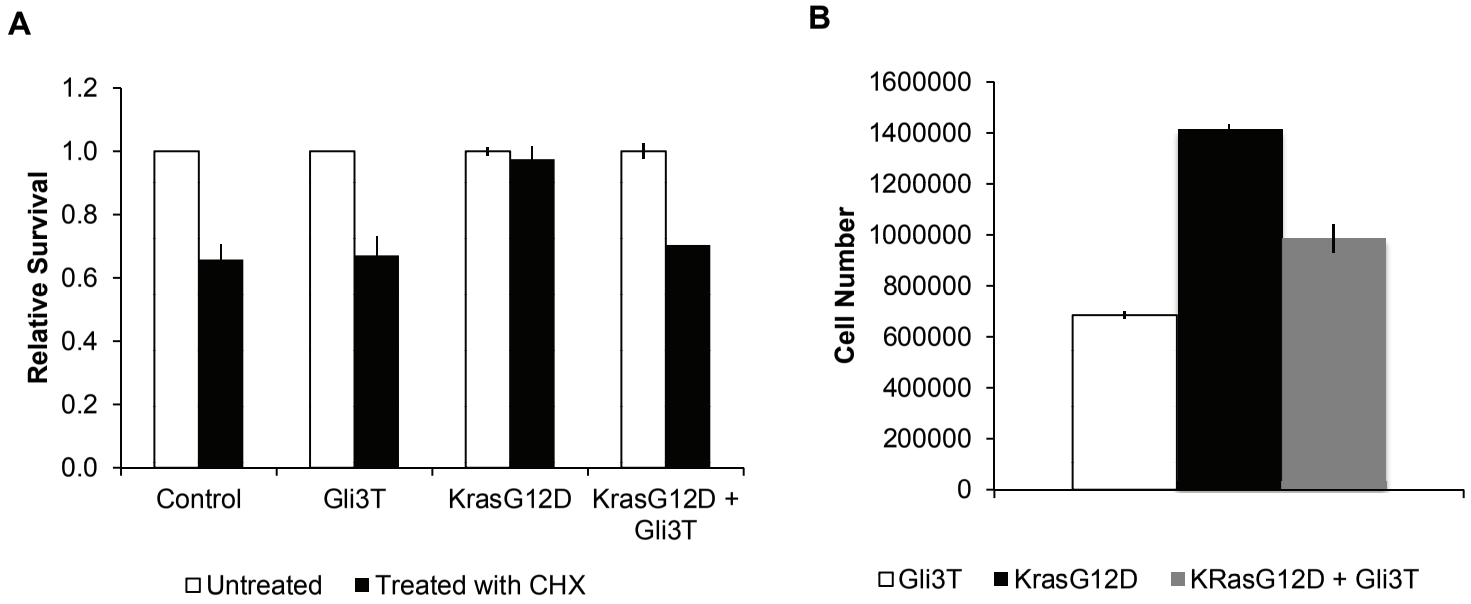
A
1.2
1.0
0.8
0.6
0.4
0.2
0.0
Relative Survival
Control
Gli3T
KrasG12D
KrasG12D + Gli3T
Untreated
Treated with CHX
B
1600000
1400000
1200000
1000000
800000
600000
400000
200000
0
Cell Number
Gli3T
KrasG12D
KRasG12D + Gli3T

Figure S1

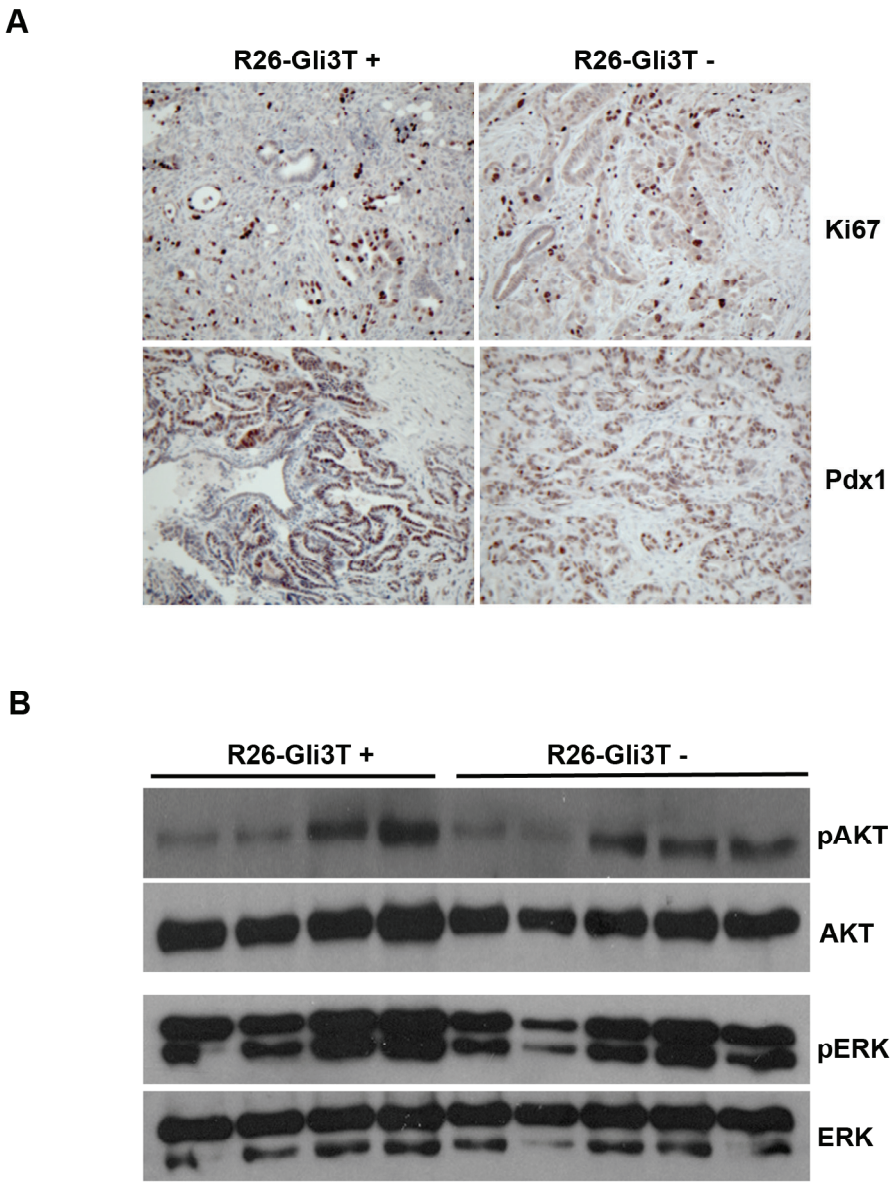
A
R26-Gli3T +
R26-Gli3T -
Ki67
Pdx1
B
R26-Gli3T +
R26-Gli3T -
pAKT
AKT
pERK
ERK

Figure S2

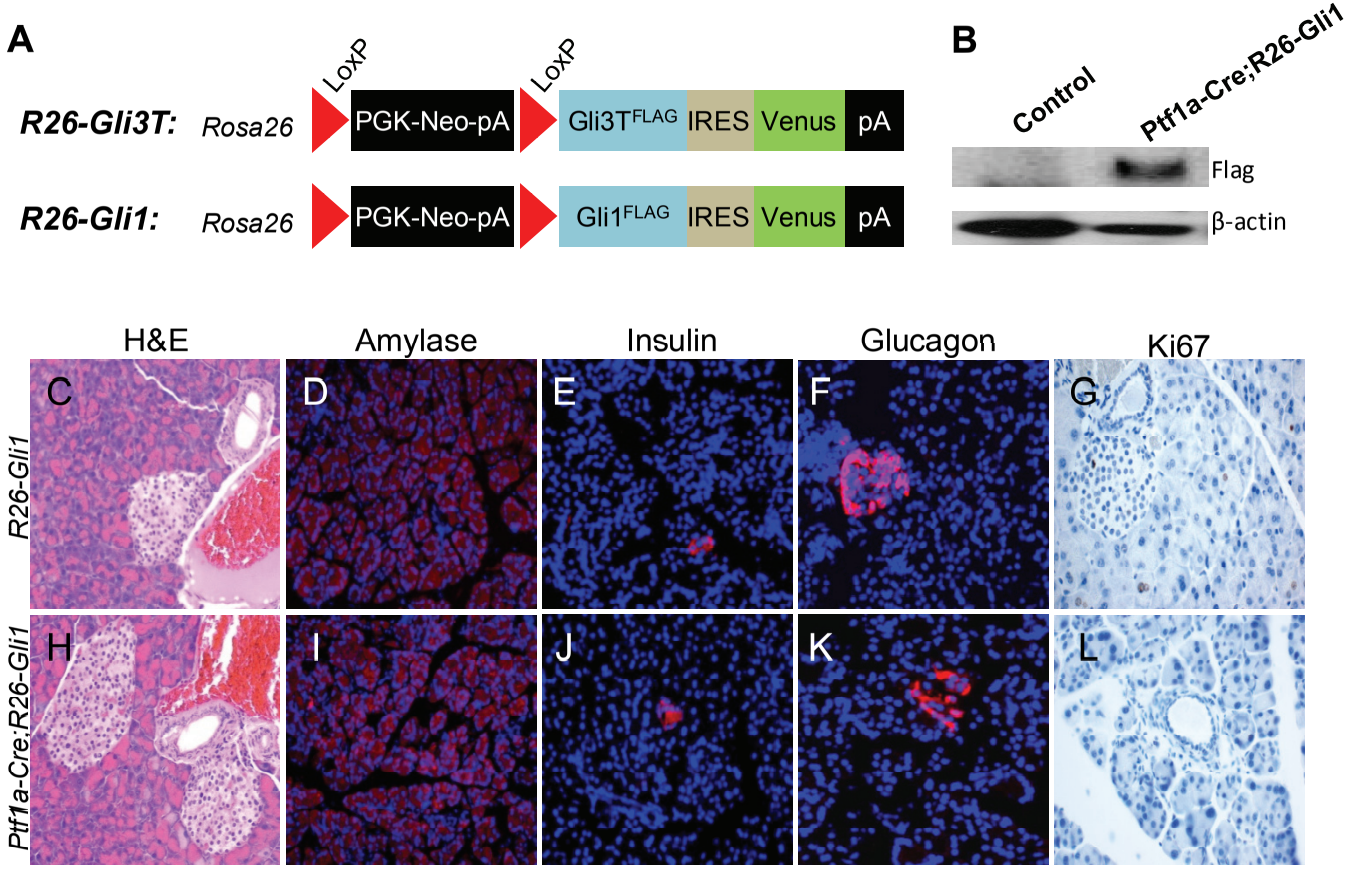
A
LoxP
LoxP
R26-Gli3T:
Rosa26
PGK-Neo-pA
Gli3T^FLAG
IRES
Venus
pA
R26-Gli1:
Rosa26
PGK-Neo-pA
Gli1^FLAG
IRES
Venus
pA
B
Control
Ptf1a-Cre;R26-Gli1
Flag
β-actin
H&E
Amylase
Insulin
Glucagon
Ki67
R26-Gli1
Ptf1a-Cre;R26-Gli1
C
D
E
F
G
H
I
J
K
L

Figure S3

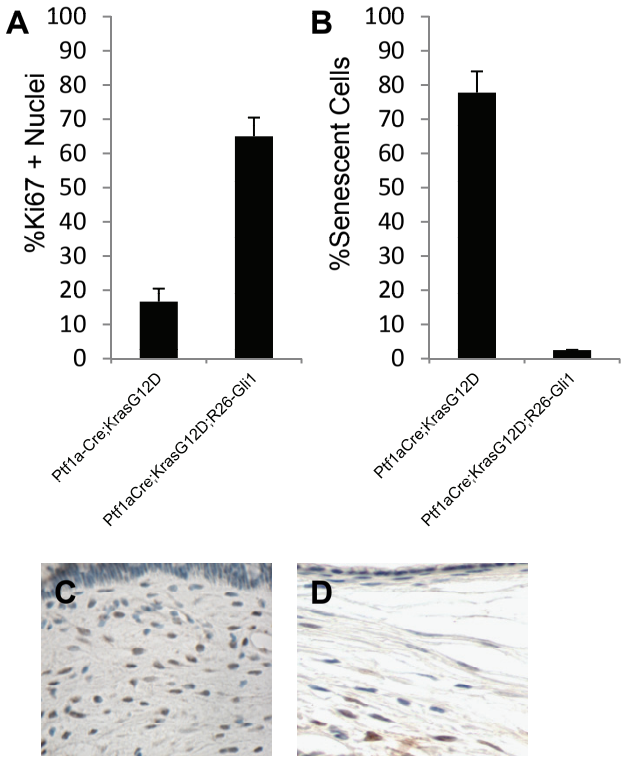
A
%Ki67 + Nuclei
100
90
80
70
60
50
40
30
20
10
0
Ptf1a-Cre;KrasG12D
Ptf1aCre;KrasG12D;R26-Gli1
B
%Senescent Cells
100
90
80
70
60
50
40
30
20
10
0
Ptf1aCre;KrasG12D
Ptf1aCre;KrasG12D;R26-Gli1
C
D

Figure S4

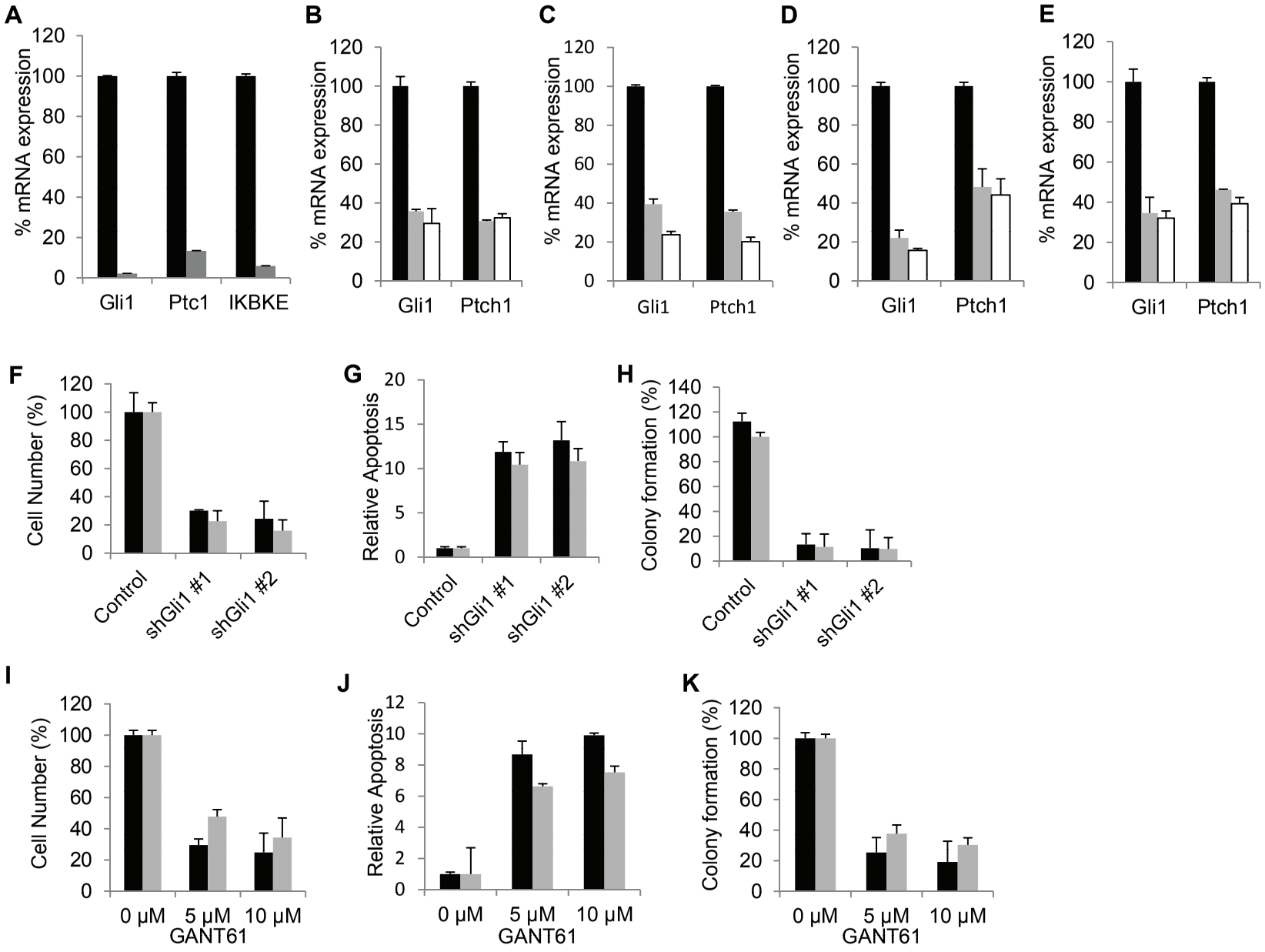
A
% mRNA expression
120
100
80
60
40
20
0
Gli1
Ptc1
IKBKE
B
% mRNA expression
Gli1
Ptch1
C
% mRNA expression
Gli1
Ptch1
D
% mRNA expression
Gli1
Ptch1
E
% mRNA expression
Gli1
Ptch1
F
Cell Number (%)
Control
shGli1 #1
shGli1 #2
G
Relative Apoptosis
20
15
10
5
0
Control
shGli1 #1
shGli1 #2
H
Colony formation (%)
140
120
100
80
60
40
20
0
Control
shGli1 #1
shGli1 #2
I
Cell Number (%)
0 μM
5 μM
10 μM
GANT61
J
Relative Apoptosis
12
10
8
6
4
2
0
0 μM
5 μM
10 μM
GANT61
K
Colony formation (%)
0 μM
5 μM
10 μM
GANT61

Figure S5

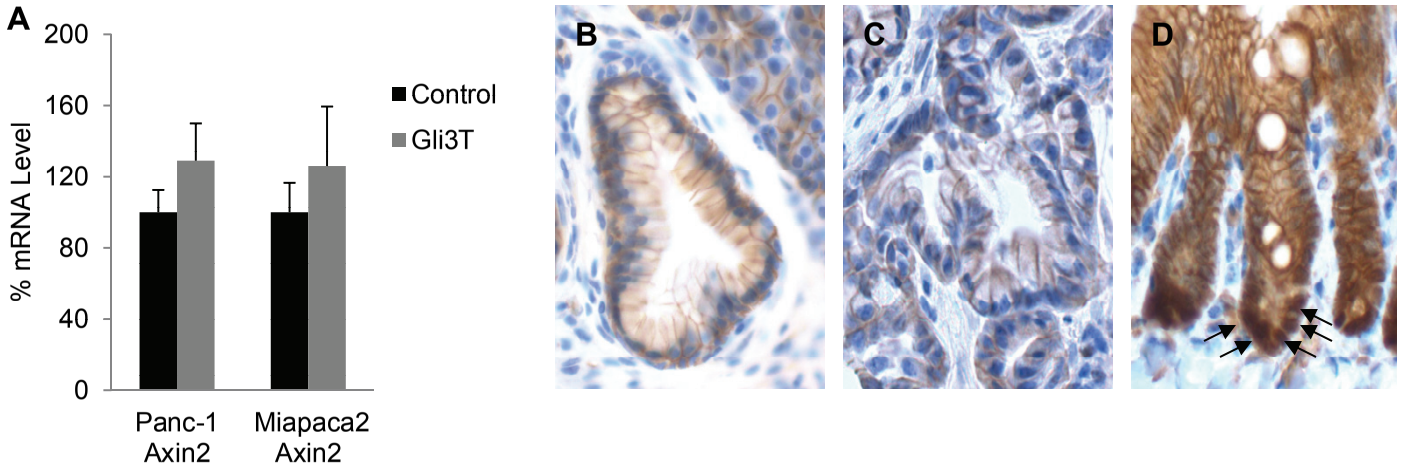
A
200
160
120
80
40
0
% mRNA Level
Control
Gli3T
Panc-1
Axin2
Miapaca2
Axin2
B
C
D

Figure S6

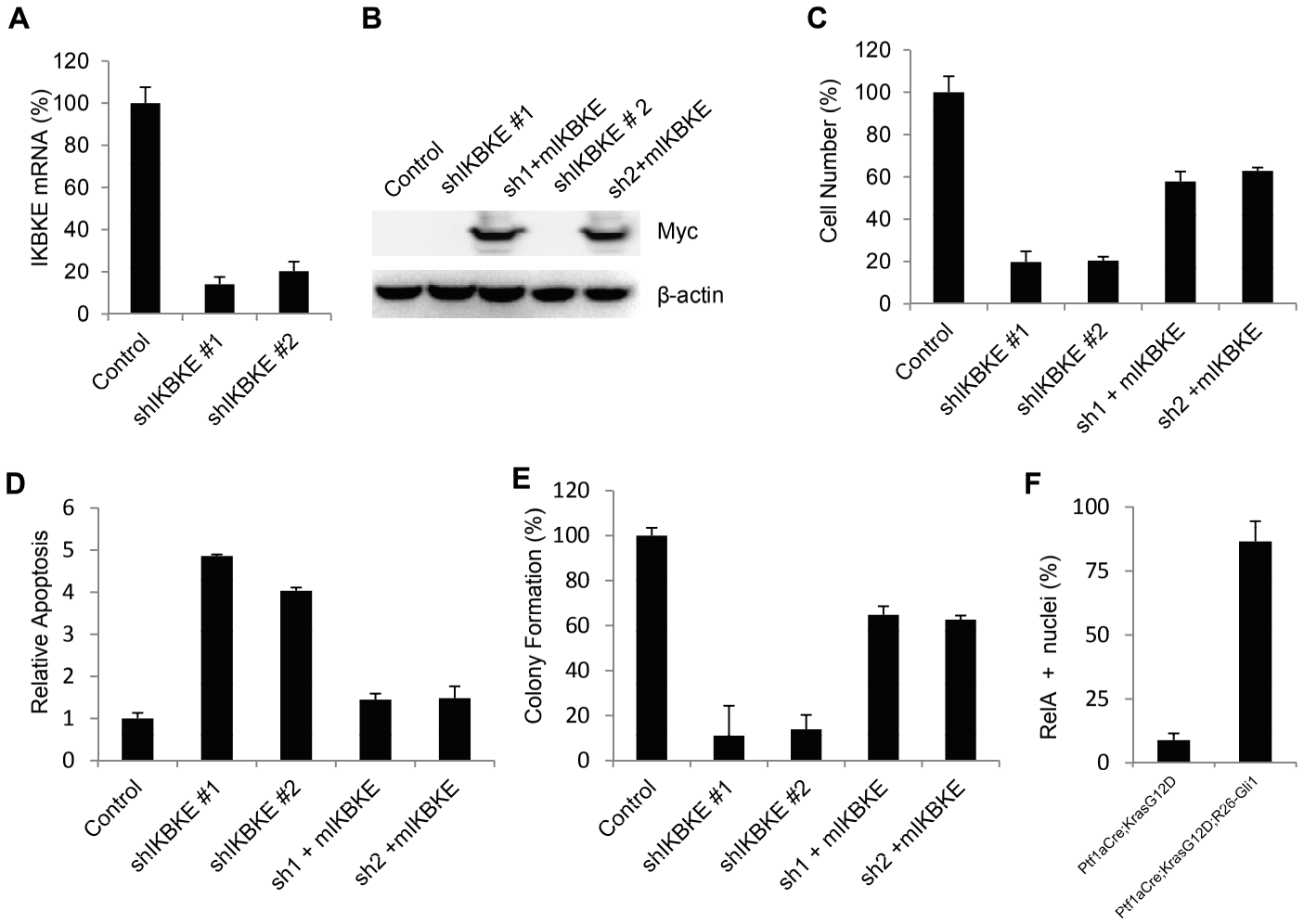
A
IKBKE mRNA (%)
120
100
80
60
40
20
0
Control
shIKBKE #1
shIKBKE #2
B
Control
shIKBKE #1
sh1+mIKBKE
shIKBKE # 2
sh2+mIKBKE
Myc
β-actin
C
Cell Number (%)
120
100
80
60
40
20
0
Control
shIKBKE #1
shIKBKE #2
sh1 + mIKBKE
sh2 +mIKBKE
D
Relative Apoptosis
6
5
4
3
2
1
0
Control
shIKBKE #1
shIKBKE #2
sh1 + mIKBKE
sh2 +mIKBKE
E
Colony Formation (%)
120
100
80
60
40
20
0
Control
shIKBKE #1
shIKBKE #2
sh1 + mIKBKE
sh2 +mIKBKE
F
RelA + nuclei (%)
100
75
50
25
0
Ptf1aCre;KrasG12D
Ptf1aCre;KrasG12D;R26-Gli1

Figure S7